Passive-Set-Position-Modulation Framework for Interactive Robotic Systems

Dongjun Lee, *Member, IEEE*, and Ke Huang

Abstract—**In this paper, we propose a novel framework, passive set-position modulation (PSPM), which enables us to connect a (continuous-time) robot's position to a sequence of slowly updating/sparse (discrete-time) set-position signal via the simple (yet frequently used in practice) spring coupling with damping injection, while enforcing passivity of the closed-loop robotic system. The PSPM modulates the original set-position signal in such a way that the modulated signal is as close to the original signal as possible (i.e., maximum information recovery for better performance), yet only to the extent permissible by the available energy in the system (i.e., passivity constraints). We present its algorithm and theoretically show its passivity and performance. We also show how this PSPM can be applied for two applications, with some experimental results: Internet teleoperation with varying delay and packet loss; and haptics with slow and variable-rate data update.**

Index Terms—**Hybrid system, Internet teleoperation, passivity, position feedback, variable-rate haptics.**

I. Introduction

LET US consider a robotic system that is mechanically interacting with humans/environments and whose continuous-time (which is henceforth referred to as continuous) position $x(t) \in \Re^n$ is desired to follow a certain sequence of slowly-updating/sparse discrete-time (which is henceforth referred to as discrete) set-position signal $y(k) \in \Re^n$, which is possibly nonuniformly updated/received at time t_k, with $k \in \{0, 1, 2, \ldots\}$ being its discrete-time index (see Fig. 1). Let us also suppose that the set-position signal $y(k)$ is directly connected to the robot's position $x(t)$ via the spring coupling $K(x(t) - y(k))$ with damping injection $B\dot{x}(t)$, aiming to regulate $\|x(t) - y(k)\|$ during the operation, where $\| \star \| = \sqrt{\star^T \star}$ is the Euclidean norm. Also, assume that the robot's local servo rate is fast enough and that the update rate of $y(k)$ is slow enough so that the spring coupling $K(x(t) - y(k))$ and the damping injection $B\dot{x}(t)$ can be considered to be continuous signals [4], [5], with $y(k)$ being the only discrete signal in them.

Manuscript received October 23, 2009; revised January 23, 2010. First published March 1, 2010; current version published April 7, 2010. This work was supported in part by the National Science Foundation under Grant CMMI-0727480 and in part by the College of Engineering, University of Tennessee. This paper was presented in part at HAPTICS, Reno, NV, March 2008; HAPTICS, Salt Lake City, UT, March 2009; and the IEEE/Robotics Society of Japan International Conference on Intelligent Robots and Systems, St. Louis, MO, October 2009. This paper was recommended for publication by Associate Editor N. Y. Chong and Editor K. Lynch upon evaluation of the reviewers' comments.

The authors are with the Department of Mechanical, Aerospace and Biomedical Engineering, University of Tennessee, Knoxville, TN 37996 USA (e-mail: djlee@utk.edu; khuang1@utk.edu).

Color versions of one or more of the figures in this paper are available online at http://ieeexplore.ieee.org.

Digital Object Identifier 10.1109/TRO.2010.2041877

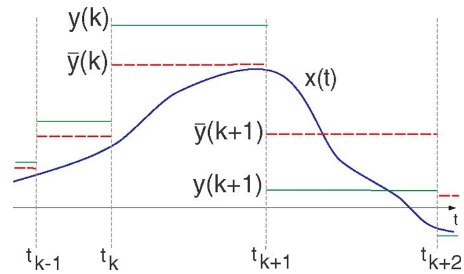

Fig. 1. Robot's continuous position $x(t)$, discrete set-position signal $y(k)$, which is received at t_k, and its modulated version $\bar{y}(k)$.

This description is pertinent to some important applications in robotics: 1) bilateral teleoperation over the Internet, particularly when the master and slave robots' positions are connected via the spring coupling with damping injection [4], [6] over the (discrete) Internet, with severe varying delay and packet loss so that their set-position updates are either slow or only sparse; 2) haptics with the (discrete) information-update rate for the virtual coupling [7] from the virtual-world simulation being much slower with respect to (w.r.t.) the device's servo rate and, possibly, nonuniform (e.g., virtual environment on a remote PC that is connected via slow/unreliable Internet; complex deformable object with intermittent multipoint contacts [8]); and 3) a material handling robot in a factory, whose set-position command is sent from a central server via a slow/imperfect wireless local area network (WLAN), to name a few.

For these applications, the foremost requirement is the interaction (or coupled) stability [9] of the robot with a wide range of humans/environments, whose dynamics are usually either unknown, uncertain, and/or too complicated to be captured by a mathematically tractable model. For this, the concept of passivity has been utilized in numerous works (e.g., [6] and [9]–[14]), i.e., by rendering the closed-loop robot to be passive, its interaction with *any* passive humans/environments is guaranteed to be stable, regardless of the structure, complexity, and parameters of the dynamics of the humans and environments.

At the same time, to attain an adequate level of performance, it is often critical to maintain the coordination between $x(t)$ and $y(k)$ (e.g., perceive a wall contact of $y(k)$ by maintaining $\|x(t) - y(k)\|$ to be small). For this, the simple spring coupling K with damping injection is used frequently in practice to connect the robot's position $x(t)$ and the set-position signal $y(k)$ [4], [15]. Yet, this is usually done without enough (or any) theoretical justification (e.g., stability guarantee), and it is well known that, particularly when the discrete sequence of $y(k)$ is either updated slowly/nonuniformly and/or embeds varying delay/packet loss in it, this spring coupling can easily become unstable, thus suggesting that passivity should be broken down as well.

In this paper, we provide a solution to this problem, i.e., how to enforce passivity of such a (continuous) spring coupling K (with damping injection) between the robot's continuous position $x(t)$ and a slowly updating/sparse switching sequence of discrete set-position signal $y(k)$. More precisely, first, relying on the intrinsic passivity [12] of the continuous robot's dynamics and the spring connection (with injected damping), we show that the reason for possible violation of passivity in this scenario is jumping in the spring potential energy at each data-reception (or switching) instance t_k. Then, to passify this possibly passivity-breaking energy jump, we propose a novel framework, *passive set-position modulation* (PSPM) [1]–[3]: At each time instance t_k of receiving a new set-position data $y(k)$, we compute its modulated version $\bar{y}(k)$ in such a way that this $\bar{y}(k)$ is as close to $y(k)$ as possible (i.e., for better performance), yet only to the extent that the use of $\bar{y}(k)$ for the spring coupling K, instead of $y(k)$, is permissible by the passivity constraint.

To further enhance the performance of this PSPM algorithm, we also augment it with a virtual energy reservoir similarly to [13], [14], [16], and [17], along with the following mechanisms: 1) *energy reharvesting*, which recaptures a (substantial) portion of otherwise-wasted energy dissipation via the artificially injected damping and deposits it back into the virtual energy reservoir, thereby significantly improving the system's energy efficiency and performance [i.e., more energy to push $\bar{y}(k)$ closer to $y(k)$] and 2) *energy shuffling/ceiling*, which trims off energy accumulation of the virtual energy reservoir above a certain threshold and sends it to the communication counterpart, thereby preventing potentially dangerous excessive energy accumulation as well as emulating energy transfer of the mechanical interaction.

We also show how to apply for PSPM: 1) the Internet teleoperation with substantial loss/delay and 2) haptics with slow and variable-rate data update, along with their respective experimental results. For these applications, the PSPM theoretically guarantees passivity and performance (e.g., bounded-position coordination error), as well as provides explicit position feedback [i.e., $\bar{y}(k) = y(k)$] if doing so complies with the passivity constraint. To our knowledge, these theoretical guarantees of passivity/performance and explicit position feedback, albeit of foremost importance for the aforementioned applications, have not been achieved by other works (e.g., no passivity guarantee with either varying delay or packet loss [4], [6], [18]; position drift due to the lack of position feedback [5], [10], [19], [20]; virtual coupling whose passivity is established only for uniform update rate [7]).

Perhaps, most closely related to our PSPM framework are 1) time-domain passivity [or passivity observer/passivity controller (PO/PC)] approach [13], [21], [22]; 2) the energy-bounding algorithm (EBA) [23]; and 3) the result of [20], and it would be worth comparing these with the PSPM. First, the PO/PC approach is a "see-then-action" policy (i.e., *after* PO sees violation of passivity, PC acts to dissipate it), while the PSPM is a "preventive" one (i.e., $y(k)$ is modulated *before* violation of passivity to prevent it). An important ramification of this is that our PSPM is free from the singularity and noisy behavior of the PO/PC [24], which are the consequences of the "see-then-action" nature (i.e., if velocity becomes zero just after PO detects passivity violation, an unbounded PC is necessary to regain passivity). On the other hand, the EBA modulates the control force, while the PSPM modulates the set-position signal $y(k)$. This difference, we believe, is the main reason of why the EBA often suffers from force/position mismatches, particularly with delay/loss [25], while the PSPM does not, although exact explanation for this is not clear at this moment. Last, the main result of [20] is how to render the discrete (port-Hamiltonian) system to be passive and how to connect it to a continuous power-port while matching the power flow at their interface. This is well suited for the (discrete) wave coupling as used there, since it is (discrete) passive by itself, even with loss/delay. Yet, the result of [20] is not directly applicable here, since the spring coupling K, which we aim to use for explicit position feedback, is hybrid (i.e., it contains both discrete and continuous signals) and not (discrete) passive on its own with delay/loss.

Our PSPM is designed mainly for the case where the update of the set-position sequence $y(k)$ is slow and sparse enough w.r.t. the robot's local servo rate, as manifested by its not using derivative terms of $y(k)$, which is usually necessary to track either fast-updating or dense $y(k)$. For this case, we believe that our assumption of continuous $Kx(t)$ and $B\dot{x}(t)$ in the coupling control is not so unreasonable, although it can be removed (see Remark 1). Also, as can be seen by the experimental results in Sections IV and V, the PSPM shows surprisingly good performance, with substantial loss/delay when compared with other works (e.g., agile operation with no position/force mismatch; cf., [5], [6], [18], and [20]). This, we believe, is because 1) the PSPM modulates $y(k)$ only when necessary rather than blindly applying (conservative) passifying action all the time (cf., [5], [6], and [18]); and 2) it provides explicit position feedback (under the passivity constraint), which is crucial for the most fundamental position-coordination requirement (cf., [5] and [20]).

The PSPM framework also possesses the following properties/flexibilities that are usually not found in other passivity-enforcing schemes.

1) *Hybrid formulation*: It aims to proactively exploit the hybrid nature of the problem [i.e., continuous $x(t)$ and discrete $y(k)$]. This is in sharp contrast to most of the other works (e.g., [5], [13], [18], [19], [21], and [22]—a notable exception is [20]), where this hybrid nature is usually neglected or considered to be something necessarily detrimental.
2) *Intermediate data processing:* It allows *any* (discrete) data processing of the original sequence $y(k)$, while enforcing passivity, since the only requirement for this $y(k)$ is to be a discrete sequence. This may be used for a smoothing filter for sporadic $y(k)$, a predictor to combat with data loss/delay, or a simple densifier of $y(k)$ to improve energy-reharvesting efficiency (see Lemma 2).
3) *Locality and scalability:* Its implementation and tuning (e.g., *Z*-width [26]) can be done completely locally, with no consultation with the communication counterparts.

This locality/decentralizability would be useful for applications where scalability is demanded (e.g., a multiuser haptic collaboration on the directed Internet network).

The rest of this paper is organized as follows. Some preliminary materials are introduced, and the problem of possibly passivity-breaking spring energy jumping are discussed in Section II. The main result—i.e., the PSPM—is derived and detailed in Section III. Its applications to the bilateral teleoperation over the Internet and slow/variable-rate haptics are presented in Sections IV and V, respectively, along with experimental results. Concluding remarks, with some comments on future research, are then given in Section VI.

Norm notation: We denote the norm induced by a positive-definite and symmetric matrix $M \in \Re^{n\times n}$ by $\|x\|_M := \sqrt{x^T M x}$, where $x \in \Re^n$, and the Euclidean norm is simply denoted by $\|x\| := \sqrt{x^T x}$.

II. Preliminary

A. Setting

Let us consider the following *n*-degree-of-freedom (DOF) nonlinear robotic system:

$$M(x)\ddot{x} + C(x,\dot{x})\dot{x} = \tau + f \tag{1}$$

where $x \in \Re^n$ is the position (or configuration), $M(x) \in \Re^{n\times n}$ is the symmetric and positive-definite inertia matrix, $C(x,\dot{x}) \in \Re^{n\times n}$ is the Coriolis matrix, and $\tau \in \Re^n$ is the control torque. We assume that this robotic system is mechanically interacting with humans/environments through the power $f^T\dot{x}$, where $f \in \Re^n$ and $\dot{x} \in \Re^n$ are, respectively, the interaction force and the velocity that are shared by the robot and the humans/environments. We call such systems interactive robotic systems. Here, the gravitational force is assumed to have been canceled out by a certain local control.

Then, using the well-known skew-symmetric property of $\dot{M}(x) - 2C(x,\dot{x})$, we can easily show that the robotic system (1) possesses the open-loop (energetic) passivity: $\forall T \geq 0$

$$\int_0^T [\tau + f]^T \dot{x}\, dt = \kappa(T) - \kappa(0) \geq -\kappa(0) \tag{2}$$

where $\kappa(t) := (1/2)\|\dot{x}\|^2_{M(x)}$ is the kinetic energy. To ensure interaction stability with a wide range of possibly unknown, uncertain, and complicated humans/environments, in this paper, we aim to enforce the closed-loop (energetic) passivity of the interactive robotic system: $\forall T \geq 0$

$$\int_0^T f^T \dot{x}\, dt \geq -d^2 \tag{3}$$

where $d \in \Re$ is a bounded constant that depends on the initial condition. This inequality implies that the maximum net energy that is extractable from the closed-loop robot is always bounded and, thus, safer with which to interact.

In this paper, we also suppose that for robot (1), a (discrete) set-position signal $y(k) \in \Re^n$ is received at reception times t_k $(k = 1, 2, \ldots)$, with the reception rate being neither infinitely fast nor infinitely slow, i.e., for any $k \geq 0$

$$\eta_1 \leq t_{k+1} - t_k \leq \eta_2 \tag{4}$$

where $\eta_1, \eta_2 > 0$ are bounded constants. We also assume that neither the intervals $I_k := [t_k, t_{k+1})$ are uniform (e.g., variable rate) nor was $y(k)$ sent before $y(k+1)$ from its sending port. This enables us to accommodate a variety of communication/data-update imperfectness of $y(k)$, including variable-rate update, varying delay, packet loss, and even time-swapping.

For the interactive robotic system (1) to be useful, it is, very often, required to regulate $\|x(t) - y(k)\|$ to be small. For this, perhaps, the most frequently used way, in practice, would be to connect $x(t)$ and $y(k)$ via a local spring coupling with damping injection: For $t \in I_k = [t_k, t_{k+1})$

$$\tau(t) = -B\dot{x}(t) - K(x(t) - y(k)) \tag{5}$$

where $B, K \in \Re^{n\times n}$ are the damping and spring matrices, with each being symmetric and positive definite.[1] In this paper, we assume that the update rate of $y(k)$ is slow enough (or only sparse) w.r.t. the robot's local servo rate. Then, we may consider $y(k)$ to be a sequence of *discrete* signal, while the robotic system [e.g., $x(t)$] and the local control (5), except for $y(k)$, are considered to be *continuous* systems (see Fig. 1). Similar to [27], we also exclude the case where $x(t)$ and $\dot{x}(t)$ are not continuous, which is very unlikely to happen in practice (e.g., hard impact, yet with a local plastic deformation). Note that assuming continuity for $x, \dot{x}$ does not necessarily imply that we also assume boundedness of either $x, \dot{x}$, or $\ddot{x}$ (e.g., $x = e^t$).

It is well known that the spring–damper control in (5), which directly connects $x(t)$ and $y(k)$, can easily become unstable, particularly when the sequence $y(k)$ embeds either varying delay or packet loss. Relying on the intrinsic passivity [12] of the open-loop robotic system (1), damping B, and spring K of (5), in Section II-B, we will show that the reason for this is the energy jump in the spring K due to the switchings of $y(k)$.

B. Possibly Passivity-Breaking Spring Energy Jump

First, note that within each interval $I_k = [t_k, t_{k+1})$, with $y(k)$ acting as a step input, the closed-loop robot system (1) behaves as a passive system. More precisely, we have, by integrating (2) with (5), for any $T \in I_k = [t_k, t_{k+1})$

$$\kappa(T) + \varphi(T) = \kappa(t_k) + \varphi(t_k) - \int_{t_k}^T \|\dot{x}\|^2_B\ dt + \int_{t_k}^T f^T\dot{x}\, dt \tag{6}$$

where $\varphi(t) := (1/2)\|x(t) - y(k)\|^2_K$ is the spring potential energy. This can be reorganized into the energetic passivity (3) during I_k, with $d^2 = \kappa(t_k) + \varphi(t_k)$. Unfortunately, this intra-interval closed-loop passivity begins to break down when we combine (6) over entire operation time. This is because, at each switching instance, the spring energy $\varphi(t)$ jumps due to the

[1] The results of this paper are easily extendable to nonlinear springs, yet linear damping B is needed to use $D_{\min}(k)$ in (13).

switching of $y(k)$, i.e., in general, at t_k

$$\varphi(t_k) = \frac{1}{2}\|x(t_k) - y(k)\|_K^2 \neq \frac{1}{2}\|x(t_k) - y(k-1)\|_K^2 =: \varphi(t_k^-)$$

where $\varphi(t_k^-)$ is the spring potential energy just before the switching instance t_k.

Let us denote this spring energy jump by

$$\Delta P(k) := \varphi(t_k) - \varphi(t_k^-) \quad (7)$$

which can be either positive (i.e., breaking passivity) or negative (i.e., enforcing passivity), although there is no guarantee that this is always negative, as we desire. Let us also define the damping dissipation during $I_k = [t_k, t_{k+1})$ by

$$D(k) := \int_{t_k}^{t_{k+1}} \|\dot{x}\|_B^2 \ dt. \quad (8)$$

Then, combining (6) from $I_0 = [t_0, t_1)$, with $t_0 = 0$, to $I_N = [t_N, t_{N+1})$, we have that for all $N \geq 0$ and $T \in [t_N, t_{N+1})$

$$V(T) - V(0) - \sum_{k=1}^{N} \Delta P(k) + \sum_{k=0}^{N-1} D(k) + \int_{t_N}^{T} \|\dot{x}\|_B^2 \ dt = \int_0^T f^T \dot{x}\, dt \quad (9)$$

where $V(t) := \kappa(t) + \varphi(t)$ is the total energy. Thus, if there is no energy jumping such that $\Delta P(k) = 0$, since $D(k) \geq 0$ and $V(t) \geq 0$, we will then have the closed-loop passivity (3), with $d^2 := V(0)$. However, if we have a certain sequence of $y(k)$ that creates positive net-energy jumping such that $\sum_{k=1}^{N} \Delta P(k)$ becomes excessively large, the closed-loop passivity will break down, and the interaction stability/safety will be at risk.

This clearly shows that, with the intrinsically passive open-loop robot (1), damping B, and spring K of (5), the reason for the breaking of passivity is the spring energy jump due to the switchings of $y(k)$. In Section III, we propose a novel framework, i.e., PSPM, to passify these spring energy jumps, thereby allowing us to still use the local spring–damper control (5), but now with theoretical guarantees of the closed-loop passivity (3) and a level of performance.

III. Passive Set-Position Modulation

The main idea of the PSPM is to modulate the raw set-position[2] signal $y(k) \in \Re^n$ to its modulated version $\bar{y}(k) \in \Re^n$ in such a way that $\bar{y}(k)$ is as close to $y(k)$ as possible (i.e., performance), yet only to the extent that is permissible by the available energy in the system (i.e., passivity). We will also augment this basic modulation idea with some performance-enhancing mechanisms.

Let us start by considering the interval $I_k = [t_k, t_{k+1})$. Then, at t_k, we have (possibly passivity-breaking) energy jumping $\Delta P(k)$. However, we also have a (passivity-enforcing) damping dissipation $D(k)$ in (8). This suggests us the following modulation strategy: At each t_k

$$\min_{\bar{y}(k)} \quad \|y(k) - \bar{y}(k)\|$$
$$\text{subj.} \quad D(k) - \Delta \bar{P}(k) \geq 0$$

where

$$\Delta \bar{P}(k) := \bar{\varphi}(t_k) - \bar{\varphi}(t_k^-) \quad (10)$$

is the spring energy jump at t_k when the modulation $\bar{y}(k)$ is used with

$$\bar{\varphi}(t) := \frac{1}{2}\|x(t) - \bar{y}(k)\|_K^2 \qquad \forall t \in [t_k, t_{k+1})$$

$\bar{\varphi}(t_k) = (1/2)\|x(t_k) - \bar{y}(k)\|_K^2$, and $\bar{\varphi}(t_k^-) = (1/2)\|x(t_k) - \bar{y}(k-1)\|_K^2$. Here, the objective functions other than $\|y(k) - \bar{y}(k)\|$ may also be used. Note that the condition in the second line enforces all the energy jump to be dissipated via the damping B, thereby guaranteeing passivity.

This strategy, although serving as a starting point here, is not implementable, since, at the time t_k, to decide $\bar{y}(k)$, we need to compute $D(k)$ in (8), which requires future information, i.e., evolution of $\dot{x}(t)$ during $[t_k, t_{k+1})$. To avoid this causality problem, we slightly modify the strategy such that at each t_k

$$\min_{\bar{y}(k)} \quad \|y(k) - \bar{y}(k)\| \quad (11)$$

$$\text{subj.} \quad D(k-1) - \Delta \bar{P}(k) \geq 0 \quad (12)$$

where $D(k-1)$ is now computable at the decision time t_k. Note that the new condition (12) still enforces passivity, with the energy jump $\Delta \bar{P}(k)$ now being regulated to be less than the damping dissipation $D(k-1)$ of the previous $I_{k-1} = [t_{k-1}, t_k)$. We further refine this basic strategy as follows.

1) *Position-based computation of* $D(k)$*:* Usually, $D(k)$ is computed in (12) by numerically differentiating $x(t)$ (e.g., measured by encoder) to get $\dot{x}(t)$ and by numerically integrating $\|\dot{x}(t)\|_B^2$ over I_k, all w.r.t. the robot's local servo rate. However, this numerical procedure is, often, noise-contaminated/biased, possibly resulting in erroneous estimation of $D(k)$. This is even more so if the robot's local servo rate is fairly fast, yet the update of $y(k)$ is either slow or only sparse, as we assumed here.

   To avoid this, we will use an approximation of $D(k)$, which is a function of only $x(t)$ and, thus, can be computed without such numerical differentiation/integration. More precisely, using Cauchy–Schwartz inequality [29], [30]

$$\int_{t_k}^{t_{k+1}} |\dot{x}_i|\, dt \leq \sqrt{\int_{t_k}^{t_{k+1}} |\dot{x}_i|^2 \ dt \times \int_{t_k}^{t_{k+1}} 1\, dt}$$

   if the damping B of (5) is diagonal (for nondiagonal B, see below), we can show that

$$D(k) = \int_{t_k}^{t_{k+1}} \sum_{i=1}^{n} b_{ii}|\dot{x}_i|^2\, dt = \sum_{i=1}^{n} b_{ii} \int_{t_k}^{t_{k+1}} |\dot{x}_i|^2\, dt \geq \frac{1}{t_{k+1} - t_k} \sum_{i=1}^{n} b_{ii}(x_i^{\max}(k) - x_i^{\min}(k))^2 =: D_{\min}(k) \quad (13)$$

[2]The data $y(k)$ do not necessarily have to be position data—other types of data can also be incorporated (e.g., combination of velocity and force [28]).

where $x_i \in \Re$ is the ith component of $x \in \Re^n$, $b_{ii} > 0$ is the ith diagonal element of B, and we use the fact that $\int_{t_k}^{t_{k+1}} |\dot{x}_i| \, dt \geq x_i^{\max}(k) - x_i^{\min}(k)$, with $x_i^{\max}(k)$ and $x_i^{\min}(k)$ being the maximum and minimum of $x_i(t)$ during $I_k = [t_k, t_{k+1})$. We can still use (13) for nondiagonal B: First, similarity-transform $\dot{x}^T B \dot{x}$ in (8) to $\dot{z}^T \bar{B} \dot{z}$, with $\dot{z} \in \Re^n$ and positive-definite/diagonal $\bar{B} \in \Re^{n \times n}$ and then apply (13) to these $\dot{z}$ and $\bar{B}$.

We will use this $D_{\min}(k)$, instead of $D(k)$. As shown in Lemma 2, the error $e_D(k) := D(k) - D_{\min}(k) \geq 0$ is cubic w.r.t. the updating rate of $y(k)$; thus, by densifying the data stream $y(k)$ (e.g., smoothing, interpolation, or even simply repeating previous data), we can easily make this error e_D practically negligible.

2) *Virtual energy reservoir $E(k)$:* Suppose we start with a stationary system with zero initial energy: $\dot{x}(0) = 0$, $D(0) = 0$, and $\bar{y}(0) = x(0)$. Also suppose that $f(t) = 0$. Then, for $t \in [0, t_1)$, we have that $\tau(t) = 0$, $\dot{x}(t) = 0$, and $x(t) = \bar{y}(0)$. Now, even if we receive a signal $y(1) \neq \bar{y}(0)$ at t_1, the system will stay only where it has been with $\dot{x}(t) = 0$ and $x(t) = \bar{y}(0)$ for all $t \in I_1 := [t_1, t_2)$. This is because, from (12), with $x(t_1) = \bar{y}(0)$

$$D(0) = 0 \geq \Delta P(1) = \bar{\varphi}(t_1) - \bar{\varphi}(t_1^-) = \bar{\varphi}(t_1).$$

That is, $\bar{\varphi}(t_1) = (1/2)\|x(t_1) - \bar{y}(1)\|_K^2 = 0$, thus implying that $\bar{y}(1) = \bar{y}(0)$. Since this argument can be extended for $I_2, I_3, \ldots$, no attempt to follow the received set-position data $y(k)$ will be made whatsoever.

This "take-off" problem is because we start with zero initial energy in our disposal and, thus, cannot generate any useful (nonzero) initial control action. See [20] for a similar problem. To remedy this, similarly to [13], [14], and [16], we augment the system with a virtual energy reservoir E. More precisely, we simulate the following discrete-time dynamics of $E(k) \in \Re$: With nonzero initial $E(0) > 0$, at each t_k

$$E(k) = E(k-1) + D_{\min}(k-1) - \Delta \bar{P}(k) \geq 0 \quad (14)$$

where $D_{\min}(k)$ is defined in (13). Equation (14) means that, at each t_k, $E(k)$ will provide energy to generate $\Delta \bar{P}(k)$ [or receive energy from it, depending on the sign of $\Delta \bar{P}(k)$], while also reharvesting (substantial) portion of the damping dissipation of B via $D_{\min}(k-1)$. Note that this B dissipation is completely an artifact of the control (5), which is not due to the real interaction with humans/environments (via $f^T \dot{x}$). Thus, it is desirable to recapture this dissipation as much as possible (i.e., reduce "energy leak" $\sum e_D(k) = \sum [D(k) - D_{\min}(k)]$) for better energy efficiency (see Lemma 2).

3) *Energy shuffling/ceiling:* If the robot (1) operates in highly dissipative environments, it would be useful to send some extra energy $\Delta E_y(k) > 0$, along with $y(k)$ to the robot to recharge its $E(k)$ from time to time. However, in a teleoperation, human users often keep injecting energy into the system (to command slave robot). This can result in excessive energy accumulation in the master's side $E(k)$, which, if loosened in a short period of time, may pose a safety issue to the engaging human user. For this, it would be useful if we can send some accumulated energy from the master's side to the slave's side, and *vice versa*.

We implement this idea into the PSPM: 1) Along with $y(k)$, energy-shuffling term $\Delta E_y(k)$ is also transmitted (e.g., sent from the central server), with (14) being modified by

$$E(k) = E(k-1) + \Delta E_y(k) + D_{\min}(k-1) - \Delta \bar{P}(k) \geq 0 \quad (15)$$

and 2) if the energy of $E(k)$, after (15) is performed, is more than an upper limit $\bar{E}$ (i.e., $E(k) > \bar{E}$), we ceil it by $\bar{E}(k)$ (i.e., $E(k) \Leftarrow \bar{E}$) and send the trimmed-off energy $\Delta E_x(k) := E(k) - \bar{E}$ [along with the set-position signal $x(t_k)$] to the communication counterpart or simply discard it if such counterparts do not exist. This energy shuffling/ceiling allows the energy transfer of mechanical interaction between two systems to be emulated, even if they are physically disjoint.

Algorithm 1 Passive Set-Position Modulation

1: $\bar{y}(0) \Leftarrow x(0),\ E(0) \Leftarrow \bar{E},\ k \Leftarrow 0$
2: **repeat**
3: **if** data $(y, \Delta E_y)$ is received **then**
4: $k \Leftarrow k + 1$
5: $y(k) \Leftarrow y,\ \Delta E_y(k) \Leftarrow \Delta E_y$
6: retrieve $x(t_k),\ x_i^{\max}(k-1),\ x_i^{\min}(k-1)$
7: find $\bar{y}(k)$ by solving

$$\min_{\bar{y}(k)} \quad ||y(k) - \bar{y}(k)|| \quad (16)$$

$$\text{subj.} \quad E(k) \Leftarrow E(k-1) + \Delta E_y(k) + D_{\min}(k-1) - \Delta \bar{P}(k) \geq 0 \quad (17)$$

8: **if** $E(k) > \bar{E}$ **then**
9: $\Delta E_x(k) \Leftarrow E(k) - \bar{E},\ E(k) \Leftarrow \bar{E}$
10: **else**
11: $\Delta E_x(k) \Leftarrow 0$
12: **end if**
13: send $(x(t_k), \Delta E_x(k))$ or discard
14: **end if**
15: **until** termination

The complete PSPM algorithm is presented in Algorithm 1, where we can see that the PSPM sets the modulation $\bar{y}(k)$ as close to the raw signal $y(k)$ as possible [i.e., aiming for performance; see (16)], yet only to the extent that is permissible by the available energy in the system [i.e., enforcing passivity; see (17)]. Note that the solution of this optimization [i.e., (16)–(17)] always exists and is unique, since the feasible set of $\bar{y}(k)$ under the constraint (17) is convex, and the objective function (16) is also convex w.r.t. $\bar{y}(k)$ [31] (see Fig. 2). In Algorithm 1, we assume that the PSPM is triggered whenever a new datum $(y, \Delta E_y)$ is received (line 3). Of course, other triggering mechanisms are also possible [e.g., timed trigger, with $(y, \Delta E_y) = (y(k-1), 0)$]. It is also clear from Algorithm 1 that the implementation/tuning (e.g., choosing B, K) of the

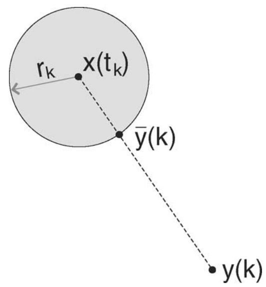

Fig. 2. Convex geometry of $x(t_k)$, $y(k)$, and $\bar{y}(k)$, with $K = \lambda I$ ($\lambda > 0$), where $r_k^2 := (2/K) \cdot [E(k-1) + \Delta E_y(k) + D_{\min}(k-1)] + \|x(t_k) - \bar{y}(k-1)\|^2$ from (17). This implies that $\exists \alpha_k \in [0,1]$ s.t. $\bar{y}(k) = \alpha_k x(t_k) + (1-\alpha_k) y(k)$. The ball $B(x(t_k), r_k)$ will become an ellipsoid if $K \neq \lambda I$.

PSPM can be done completely locally. This property would be useful for applications that demand scalability (e.g., multiuser haptic interaction over a directed Internet network, with the PSPM being installed at each user's site).

Energetics of the PSPM are also illustrated in Fig. 3, which shows that 1) PSPM computes $\bar{y}(k)$ from $y(k)$ using the reharvested energy $D_{\min}(k-1)$, the received energy $\Delta E_y(k)$, and whatever is left in the virtual reservoir energy $E(k-1)$; and 2) modulated $\bar{y}(k)$ is connected to $x(t)$ via a spring coupling K, with damping injection B. It is also clear from Fig. 3 that the PSPM can accommodate *any* intermediate data processing (at the "filter" block), while still enforcing passivity, since the PSPM block can accept any discrete switching sequence $y(k)$ as its incoming data stream, which is not necessarily only that of set-position signals. This data processing may be used either to densify the data stream for better energy efficiency (see Lemma 2) or to enhance performance (e.g., predictor/estimator), while enforcing passivity.

Theorem 1: Consider the interactive robotic system (1) under the local spring–damper control (5) and the PSPM with bounded $E(0)$. Suppose that $\dot{x}(t)$ and $x(t)$ are continuous $\forall t \geq 0$ and $\exists$ a bounded constant $b \in \Re$ s.t. $\sum_{j=1}^{k} \Delta E_y(j) \leq b^2 \ \forall k \geq 1$.

1) *Passivity/stability:* The closed-loop system is passive in the sense of (3). Also, if the human/environment is passive, i.e., $\forall T \geq 0$, $\exists$ a bounded constant $c \in \Re$ s.t.
$$\int_0^T f^T \dot{x}\, dt \leq c^2 \tag{18}$$
interaction is stable in the sense of bounded $\dot{x}(t)$ and $\|x(t) - \bar{y}(k)\|_K$.

2) *Position tracking:* Assume that $f(t) = 0$ and that the robot (1) has an unmodeled positive-definite damping B_e. Further, assume that $\exists$ bounded $\lambda_1, \lambda_2 > 0$ s.t. $\underline{\sigma}[M(x)] \geq \lambda_1$ and $|\partial M_{qr}(x)/\partial x_s| \leq \lambda_2$ for all $x \in \Re^n$, $q, r, s = 1, \ldots, n$, where $\underline{\sigma}(\star)$ is the smallest singular value of $\star$, and M_{qr}, x_s are the qrth and sth components of M and x, respectively. Then, $\dot{x}(t) \to 0$, $\|\bar{y}(k+1) - \bar{y}(k)\| \to 0$, and $\|x(t) - \bar{y}(k)\| \to 0$. Further, suppose that $\exists p \geq 0$ s.t. $E(k) > 0 \ \forall k \geq p$ and $\|y(k+1) - y(k)\| \to 0$. Then, $\|x(t) - y(k)\| \to 0$.

3) *Haptic feedback:* Suppose that $(\ddot{x}(t), \dot{x}(t), x(t)) \to (0, 0, x_o)$ and $y(k) \to y_o$, with constant $x_o, y_o \in \Re^n$, and $\exists p \geq 0$ s.t. $E(k) > 0 \ \forall k \geq p$. Then, $f(t) \to K(x_o - y_o)$.

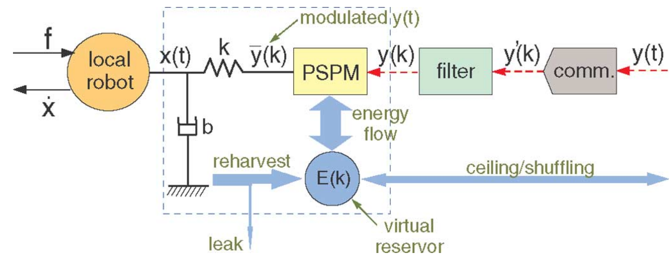

Fig. 3. Energetics of the PSPM.

Proof: For the first item, similarly to (9), with $y(k)$ in (5) replaced by $\bar{y}(k)$ and $\Delta P(k)$ in (9) replaced by $\Delta \bar{P}(k)$ of (10), and using $e_D(k) = D(k) - D_{\min}(k) \geq 0$ from (13), we can show that for all $N \geq 0$ and $T \in I_N = [t_N, t_{N+1})$, with $D(0) = 0$ and $t_o = 0$
$$\begin{aligned}\int_0^T f^T \dot{x}\, dt &= V(T) - V(0) + \sum_{k=1}^{N} [D_{\min}(k-1) - \Delta \bar{P}(k)] \\ &\quad + \sum_{k=1}^{N} e_D(k-1) + \int_{t_N}^{T} \|\dot{x}\|_B^2\, dt \\ &\geq V(T) - V(0) \\ &\quad + \sum_{k=1}^{N} [E(k) - E(k-1) - \Delta E_y(k) + \Delta E_x(k)] \\ &\geq V(T) - V(0) + E(N) - E(0) - \sum_{k=1}^{N} \Delta E_y(k)\end{aligned} \tag{19}$$
where $V(t) := \kappa(t) + \bar{\varphi}(t)$, $\bar{\varphi}(T) = (1/2)\|x(T) - \bar{y}(N)\|_K^2$, and we use the property of the energy ceiling/shuffling [(17) and lines 8–13 in Algorithm 1], i.e.,
$$\begin{aligned}&D_{\min}(k-1) - \Delta \bar{P}(k) \\ &\quad = E(k) - E(k-1) - \Delta E_y(k) + \Delta E_x(k) \\ &\quad \geq E(k) - E(k-1) - \Delta E_y(k)\end{aligned} \tag{20}$$
where the last line is because $\Delta E_x(k) \geq 0$, with $\Delta E_x(k) = 0$ only if line 8 of Algorithm 1 is false. Then, the closed-loop passivity (3) is achieved from (19), with $d^2 = V(0) + E(0) + b^2$, where $b^2 \geq \sum_{k=1}^{N} \Delta E_y(k)$, as assumed previously. Also, from (19) with (18), we have that $c^2 + d^2 \geq V(T) + E(N) \geq V(T)$, thus implying that $\dot{x}(t)$ and $\|x(t) - \bar{y}(k)\|$ are bounded $\forall t \geq 0$.

For the second item, with the additional B_e, similarly to (19), we have that $\forall N \geq 0$ and $\forall T \in I_N = [t_N, t_{N+1})$
$$\int_0^T f^T \dot{x}\, dt \geq V(T) - V(0) + E(N) - E(0) - \sum_{k=1}^{N} \Delta E_y(k) + \int_0^T \|\dot{x}\|_{B_e}^2\, dt$$

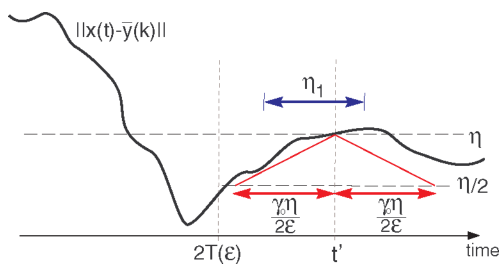

Fig. 4. I_w in the proof of item 2 of Theorem 1.

where the left-hand side (LHS) is zero, with $f = 0$. This shows that from the positive-definiteness of $V(t)$ and $B_e, \dot{x}(t), x(t) - \bar{y}(k)$ are bounded, and $\dot{x}(t)$ is square-integrable. From (1), we also have the following closed-loop dynamics:

$$M(x)\ddot{x} + C(x,\dot{x})\dot{x} + B_e\dot{x} + B\dot{x} + K(x - \bar{y}(k)) = f \quad (21)$$

where, with $f = 0$, $\ddot{x}(t)$ is also uniformly bounded, since $C(x,\dot{x})$ is linear w.r.t. $\dot{x}$ and $\partial M_{qr}/\partial x_s$, which are both bounded, and $\underline{\sigma}[M(x)] \geq \lambda_1 > 0$. Thus, from Barbalat's lemma [32], $\dot{x}(t) \to 0$; or, in other words, for any $\epsilon > 0$, $\exists$ a sufficiently large $T(\epsilon) \geq 0$ s.t. $\|\dot{x}(t)\| \leq \epsilon$ for all $t \geq T(\epsilon)$.

Now, suppose *not* $\|x(t) - \bar{y}(k)\| \to 0$. Then, we can find a time $t' > 2T(\epsilon)$ s.t. $\|x(t') - \bar{y}(k)\| > \eta$ for a positive scalar $\eta > 0$. Moreover, we have that $\|x(t) - \bar{y}(k)\| > \eta/2$ for all $t \in I_w$, where $I_w(\eta, \eta_1, \epsilon)$ is the time interval, which contains t' and is of the length $\min(\gamma_o\eta/(2\epsilon), \eta_1/2)$, with γ_o being a certain (bounded) constant that depends on the dimension n of (1). This is because $\|x(t) - \bar{y}(k)\| \leq \eta/2$ can happen only either before or after t' either due to the evolution of $x(t)$ or due to the switching of $\bar{y}(k)$, yet the former is restricted by $\|\dot{x}\| \leq \epsilon$, while the latter cannot be denser than η_1 of (4) (see Fig. 4).

During this I_w, from (21), we will then have that for a certain $q \in \{1, 2, \ldots, n\}$

$$|\ddot{x}_q(t)| \geq -\gamma_1\epsilon^2 - \gamma_2\epsilon + \gamma_3\eta \quad (22)$$

for all $t \in I_w$, where $\gamma_1, \gamma_2, \gamma_3 > 0$ are bounded constants that, respectively, come from the Coriolis term, damping terms, and $K(x - \bar{y}(k))$ of (21). This implies that by choosing ϵ to be small enough, we can always push $\dot{x}$ outside the ball $\|\dot{x}\| \leq \epsilon$ during this I_w, since, as $\epsilon \to 0$, $I_w \to \eta_1/2$, and $|\int_{I_w} \ddot{x}_q\, dt| \geq (\gamma_3\eta - \gamma_1\epsilon^2 - \gamma_2\epsilon)\eta_1/2 \to \gamma_3\eta\eta_1/2 \gg \epsilon$, where, with a slight abuse of notation, we use I_w to denote its length. This contradicts the fact that $\|\dot{x}(t)\| \leq \epsilon\ \forall t \geq T(\epsilon)$. Therefore, $\|x(t) - \bar{y}(k)\| \to 0$. With $\dot{x}(t) \to 0$, this implies that $\|\bar{y}(k+1) - \bar{y}(k)\| \to 0$. Moreover, if we have that $E(k) > 0$ for all $k \geq p$ with a bounded $p \geq 0$, $\bar{y}(k) = y(k)\ \forall k \geq p$. Thus, $\|x(t) - \bar{y}(k)\| \to 0$ implies that $\|x(t) - y(k)\| \to 0$, with a necessary condition for this, i.e., $\|y(k+1) - y(k)\| \to 0$, is granted *a priori* by the assumption.

The third item is a direct consequence of the closed-loop dynamics (21): With $(\ddot{x}(t), \dot{x}(t)) \to 0$ and $(x(t), \bar{y}(k)) \to (x_o, y_o)$, we have that $f(t) \to K(x_o - y_o)$. ■

The assumptions that $f = 0$ for item 2 and $(\ddot{x}(t), \dot{x}(t)) \to 0$ for item 3 of Theorem 1 are made here to reflect the situations in which the robot is released from the environment/human and makes a hard contact with them, respectively. The assumptions that $\underline{\sigma}[M(x)] \geq \lambda_1 > 0$ and $|\partial M_{qr}/\partial x_s| \leq \lambda_2$ in item 2 of Theorem 1, which are satisfied by many practical robotic systems (e.g., revolute joint robots [32]), are used here to attain the boundedness of $\ddot{x}$ from (21) (to show that $\dot{x} \to 0$ using Barbalat's lemma) and the inequality (22). Any other conditions for the robots (1), which can provide similar properties, can replace these assumptions.

Item 2 of Theorem 1 says that if the robot (1) is released (with $f = 0$) and the energy input to it [i.e., $\Delta E_y(k)$] is cut off, the robot will eventually stop. This (desirable) stabilizing action of the PSPM is, in fact, due to its passivity property (item 1 of Theorem 1), i.e., the PSPM regulates the system's total energy to be bounded, while B_e keeps shedding/dissipating it (if $\dot{x} \neq 0$). Of course, here, the robot's stopping position may not be the same as the desired set position, since, under the PSPM, we may have that $\bar{y}(k) \neq y(k)$ if $E(k) = 0$ (i.e., $E(k)$ depletes energy). It is even possible that although $y(k)$ is moving, $\bar{y}(k)$ may not move, if the energy for $\bar{y}(k)$ to follow $y(k)$ is not enough (e.g., $r_k = 0$ with fixed $x(t_k)$ in Fig. 2).

This (steady-state) mismatch between the stopping position $\bar{y}(k)$ and the set position $y(k)$ is yet not so likely to happen in practice, since $\Delta E_y(k)$ (or other energy injection as captured by $D_{\min}(k)$, e.g., human energy injection in teleoperation/haptics) is usually not completely cut off. Neither have we observed so far this mismatch from our (extensive) tests of PSPM, even during the most favorable for this (e.g., intentionally destabilizing experiment of Fig. 7). Although we do not have a precise mathematical statement for this, we can, instead, show that, under some mild conditions, the position error $\|x(t) - y(k)\|$ under the PSPM is, indeed, bounded.

Lemma 1: Consider the interactive robotic system (1) with the local control (5) and the PSPM with bounded $E(0)$. Suppose that $\dot{x}(t)$ and $x(t)$ are continuous; $\sum_{j=1}^{k} \Delta E_y(j)$ is bounded $\forall k \geq j$; and the human/environment is passive in the sense of (18). Also, assume that $K = \lambda I$ with $\lambda > 0$ for (5).

1) Suppose that $\exists p \geq 0$ s.t. $\|x(t_p) - y(p)\|$ is bounded and $y(k) = y_o\ \forall k \geq p$. Then, $\|x(t) - y_o\|$ is bounded $\forall t \geq t_p$.
2) Suppose the following hold.
   a) $\exists\ y_*(t) \in \Re^n$ s.t. $y_*(t_k) = y(k)$ with bounded $\ddot{y}_*(t), \dot{y}_*(t)$.
   b) f in (1) is bounded.
   c) $\|x(t_1) - y(1)\|$ is small enough.
   d) The conditions on $\underline{\sigma}[M]$ and $\partial M_{qr}/\partial q_s$ of item 2 of Theorem 1 hold.
   e) For α_k in Fig. 2, $\exists$ a small $\epsilon_\alpha > 0$ s.t. $\alpha_k \geq 1 - \epsilon_\alpha$ happens only boundedly many times $n_\alpha \geq 0$.

Then, $\exists\ \bar{\eta}_1$ s.t. if $\eta_1 \geq \bar{\eta}_1$ for (4), $\|x(t) - y(k)\|$ is bounded $\forall t \geq 0$.

Proof: First, note that for any $k \geq 0$

$$\|y(k) - \bar{y}(k)\| \leq \|y(k) - \bar{y}(k-1)\|$$

since the optimization (16)–(17) always has $\bar{y}(k) = \bar{y}(k-1)$ as its trivial solution [with $\Delta\bar{P}(k) = 0$ in (17)]. By setting $y(k) = y_o$ for $k \geq p$, we have that $\|y_o - \bar{y}(k)\| \leq \|y_o - \bar{y}(p)\| \forall k \geq p$, and, subsequently, for any $k \geq p$

$$\|x(t_k) - y_o\| \leq \|x(t_k) - \bar{y}(k)\| + \|\bar{y}(k) - y_o\|$$
$$\leq \|x(t_k) - \bar{y}(k)\| + \|\bar{y}(p) - y_o\|$$

where the term $\|x(t_k) - \bar{y}(k)\|$ is bounded (item 1 of Theorem 1), and the last term is also bounded with $\|\bar{y}(p) - y_o\| = \alpha_p \|x(t_p) - y_o\| \leq \|x(t_p) - y(p)\|$, with $\alpha_p \in [0, 1]$, as shown in Fig. 2. Boundedness of $\|x(t) - y(k)\|$ then follows from $\|x(t) - x(t_k)\| \leq \eta_2 \|\dot{x}\|$, with bounded $\|\dot{x}\|$ (item 1 of Theorem 1) and η_2 in (4).

For the second item, define $e(t) := x(t) - y_*(t)$. Then, using (21), with $\bar{y}(k) = \alpha_k x(t_k) + (1 - \alpha_k) y(k)$, (4), and the fact that $\dot{x}$ and $\dot{y}_*$ are both bounded (item 1 of Theorem 1), we can obtain the following dynamics of $e(t)$: For $t \in I_k$

$$M\ddot{e} + C\dot{e} + B\dot{e} + (1 - \alpha_k) K e = f + g(\ddot{y}_*, \dot{y}_*, \|\dot{x}\|, \eta_2) \quad (23)$$

where g defines a bounded disturbance, with $\|g\| \leq \bar{\sigma}[M]\|\ddot{y}_*\| + (\bar{\sigma}[C] + \bar{\sigma}[B] + \eta_2 \bar{\sigma}[K])\|\dot{y}_*\| + \eta_2 \bar{\sigma}[K]\|\dot{x}\|$. Then, from the well-known fact about the Lagrangian systems [33], if $\alpha_k < 1 - \epsilon_\alpha$, there exists a quadratic Lyapunov function $W_k(e, \dot{e}) \geq 0$ s.t. for $t \in I_k$

$$\frac{dW_k}{dt} \leq -\gamma_k W_k + \rho_k \sqrt{W_k} (\|f\| + \|g\|)$$

where $\gamma_k, \rho_k > 0$ are some bounded constants. We can then see that $\dot{W}_k < 0$ whenever $W_k > d_k := [(\rho_k/\gamma_k) \cdot (\|f\| + \|g\|)]^2$ (i.e., ultimate boundedness [32]). Moreover, if $W_k \geq \bar{A} := (1 + \epsilon_d)^2 \bar{d} \geq (1 + \epsilon_d)^2 d_k$, where $\bar{d} \geq d_k \; \forall k$ and $\epsilon_d > 0$ is a positive constant, $\dot{W}_k \leq -\gamma_k \epsilon_d (1 + \epsilon_d) d_k \leq -c_w$, where $c_w := \gamma \epsilon_d (1 + \epsilon_d) d > 0$, with $\gamma, d > 0$ are defined s.t. $\gamma_k \geq \gamma > 0$, and $d_k \geq d > 0 \; \forall k$ (i.e., c_w is the slowest decreasing rate of W_k when $W_k \geq \bar{A}$). Also, for any k, p s.t. $\alpha_k < 1 - \epsilon_\alpha$ and $\alpha_p < 1 - \epsilon_\alpha$, we have that $W_k \leq (1 + \epsilon_w) W_p$ and that

$$a_1 \|e(t)\|^2 + b_1 \|\dot{e}(t)\|^2 \leq W_k(t) \leq a_2 \|e(t)\|^2 + b_2 \|\dot{e}(t)\|^2$$

for some bounded constants $\epsilon_w, a_1, a_2, b_1, b_2 \geq 0$.

First, suppose that $\alpha_k < 1 - \epsilon_\alpha$ for all $k \geq 1$. Then, if $W_{k-1}(t_{k-1}) \leq \bar{A}$ (with $k \geq 2$), $W_{k-1}(t_k) < \bar{A}$, since W_{k-1} strictly decreases whenever $W_{k-1} \geq \bar{A}$. Yet, at t_k, with the switching of $(1 - \alpha_k) K e$ in (23), the error measure $W_k(t_k)$ may jump up from $W_{k-1}(t_k) \leq \bar{A}$. This, however, is still bounded by $W_k(t_k) < (1 + \epsilon_w) \bar{A}$. Thus, by choosing $\bar{\eta}_1 = \epsilon_w \bar{A}/c_w$ (i.e., dwell time [34]), we can enforce that $W_k(t_{k+1}) \leq \bar{A}$, since $W_k(t_{k+1}) \leq \min[\bar{A}, (1 + \epsilon_w)\bar{A} - c_w \bar{\eta}_1]$, with W_k decreasing faster than c_w if $W_k \geq \bar{A}$. Also, recall that $\|e(t_1)\| = \|x(t_1) - y(1)\|$ is small and that $\|\dot{e}(t)\| = \|\dot{x}(t) - \dot{y}_*(t)\|$ is bounded $\forall t \geq 0$. Thus, we can find a large-enough ϵ_d s.t. $W_1(t_1) \leq (1 + \epsilon_d)^2 \bar{d} =: \bar{A}$, and, by setting $\bar{\eta}_1$ accordingly, we have that $W_k(t_{k+1}) \leq \bar{A} \; \forall k \geq 1$, which, in turn, implies that $\|x(t) - y(k)\|$ is bounded $\forall t \geq 0$ (with bounded $\dot{x}, \dot{y}_*$, and η_2).

Now, assume that we have some occasions of $\alpha_k \geq 1 - \epsilon_\alpha$. Then, the spring action $(1 - \alpha_k) K e$ in (23) may become ineffective, and $\|e\|$ may grow. Although this growth of $\|e\|$ is still bounded (with $\|\dot{e}\|, \eta_2$, and n_α all being bounded), it may be amplified by subsequent switchings of the spring action $(1 - \alpha_k) K e$, with $\alpha_k < 1 - \epsilon_\alpha$. To avoid this, we increase the dwell time s.t. $\bar{\eta}_1 := \epsilon_w \bar{B}/c_w$, where $\bar{B} := a_2 (\sqrt{\bar{A}/a_1} + n_\alpha c_x \eta_2)^2 + b_2 c_x^2$, with $\|\dot{e}\| \leq c_x$. To see why we choose this, let us first consider the worst-case expansion of W_k, i.e., $W_{k-1}(t_k) = \bar{A}$, with $\alpha_p \geq 1 - \epsilon_\alpha$, for $p = k, \ldots, k + n_\alpha - 1$. Then, we have that $\|e(t_k)\| \leq \sqrt{\bar{A}/a_1}$ and that $\|e(t_{k+n_\alpha})\| \leq \sqrt{\bar{A}/a_1} + c_x n_\alpha \eta_2$, where $c_x \geq \|\dot{e}(t)\| \; \forall t \geq 0$. Using W_{k-1} to measure $(\dot{e}, e)$ at t_{k+n_α}, we also have that $W_{k-1}(t_{k+n_\alpha}) \leq \bar{B}$. Moreover, with $\alpha_{k+n_\alpha} < 1 - \epsilon_\alpha$, $W_{k+n_\alpha}(t_{k+n_\alpha+1}) \leq (1 + \epsilon_w)\bar{B} - c_w \bar{\eta}_1 \leq \bar{B}$, where $\bar{\eta}_1 = \epsilon_w \bar{B}/c_w$. Thus, $\|e(t)\|$ is bounded, and so is $\|x(t) - y(k)\|$, with bounded $\dot{x}, \dot{y}_*$.

This argument also applies to nonsuccessive occasions of $\alpha_k \geq 1 - \epsilon_\alpha$, since, for this case, the expansion of W_k is less than $\bar{B}$; thus, $\bar{\eta}_1 = \epsilon_w \bar{B}/c_w$ still guarantees no amplification of W_k due to the spring switchings. ∎

The first item of Lemma 1 is for the case of hard contact in teleoperation/haptics, where the position of the slave robot (or virtual proxy), often, become stationary, while the second item says that, with a reasonable amount of energy in the system (with $r_k \neq 0$ in Fig. 2), if the switching of $\bar{y}(k)$ is slow enough (i.e., dwell time [34]), due to the attracting action of K, the position error will be bounded. Here, note that $r_k \approx 0$ (i.e., $\alpha_k \approx 1$) requires that $E(k-1)$, $\Delta E_y(k)$, $D_{\min}(k-1)$, and $\|x(t_k) - \bar{y}(k-1)\|$ are all very small, which is not likely to happen in teleoperation/haptics, particularly since the human operators usually keep injecting energy into the system. Also, the existence of y_* would be granted for teleoperation/haptics if the PSPM is installed both at the master's and slave's sides to ensure that the system behaves well (see Sections IV and V).

Note that the PSPM's convex geometry (see Fig. 2) and passivity property (see item 1 of Theorem 1 with bounded $\dot{x}$) are pivotal for Lemma 1. We can also duplicate Lemma 1 for $K \neq \lambda I$, if $\|\cdot\|$ in (16) is replaced by $\|\cdot\|_K$. The dwell time $\bar{\eta}_1$ of item 2, although it can be made small by large-enough γ_k (e.g., large B, K) and ϵ_d (since $\bar{\eta}_1 \to (\epsilon_w a_2 \bar{d})/(\gamma a_1 d)$ as ϵ_d becomes large), is conservative, and to make it substantially tighter for our nonlinear second-order dynamics (23) with unstructured switching would require significant advances in the hybrid systems theory [34], which is beyond the scope of this paper.

Note that the dissipation $D(k)$ is through the (artificial) control damping B in (5), rather than through the real robot–environment/human interaction via $f^T \dot{x}$. Thus, we want to minimize this internal-energy dissipation. By doing this, we will be able to improve energy efficiency and attain better performance [i.e., more available energy in the system (17) to push $\bar{y}(k)$ closer to $y(k)$ in (16)]. One way to achieve this is to improve the energy-reharvesting efficiency by reducing the "energy leak" $\sum e_D(k) = \sum [D(k) - D_{\min}(k)]$ (see Fig. 3). Lemma 2, along with the paragraph immediately ensuing it, shows that this energy leak can be made practically negligible by densifying the data stream $y(k)$.

Lemma 2: The energy-reharvesting error $e_D(k) = D(k) - D_{\min}(k) \geq 0$ is cubic w.r.t. the data-reception rate $\Delta t_k := t_{k+1} - t_k$, if $\ddot{x}(t)$ is bounded.

Proof: Here, we prove only for the diagonal B, since the same proof can be applied for the nondiagonal B after using the (diagonalizing) similarity transform, as stated in the argument after (13). Consider $I_k = [t_k, t_{k+1})$. Then, using the following kinematic relations: For $s, t \in I_k$

$$\dot{x}(s) = \dot{x}(t_k) + \int_{t_k}^{s} \ddot{x}(r)\, dr$$

$$\begin{aligned} x(t) &= x(t_k) + \int_{t_k}^{t} \dot{x}(s)\, ds \\ &= x(t_k) + \dot{x}(t_k)(t - t_k) + \int_{t_k}^{t} \int_{t_k}^{s} \ddot{x}(r) dr\, ds \end{aligned}$$

we can rewrite (8) s.t.

$$D(k) = \int_{I_k} \dot{x}^T(s) B \dot{x}(s) ds = \int_{I_k} \left\| \int_{t_k}^{s} \ddot{x}(r) dr + \dot{x}(t_k) \right\|_B^2 ds$$

and from (13), we can show that

$$\begin{aligned} D_{\min}(k) &\geq \frac{1}{\Delta t_k} \sum_{i=1}^{n} b_{ii} (x_i(t_{k+1}) - x_i(t_k))^2 \\ &= \frac{1}{\Delta t_k} \| x(t_{k+1}) - x(t_k) \|_B^2 \\ &= \frac{1}{\Delta t_k} \left\| \dot{x}(t_k) \Delta t_k + \int_{I_k} \int_{t_k}^{s} \ddot{x}(r) dr\, ds \right\|_B^2 \end{aligned}$$

since $(x_i^{\max}(k) - x_i^{\min}(k))^2 \geq (x_i(t_{k+1}) - x_i(t_k))^2$. Combining these, we can then obtain

$$\begin{aligned} &D(k) - D_{\min}(k) \\ &\quad \leq \int_{I_k} \left\| \int_{t_k}^{s} \ddot{x}(r) dr \right\|_B^2 ds - \frac{1}{\Delta t_k} \left\| \int_{I_k} \int_{t_k}^{s} \ddot{x}(r) dr\, ds \right\|_B^2 \\ &\quad \leq \frac{1}{3} a_{\max}^2 \bar{\sigma}[B] \Delta t_k^3 \end{aligned} \tag{24}$$

where $a_{\max} \geq \|\ddot{x}(t)\|$ for all $t \geq 0$, and $\bar{\sigma}[B]$ is the maximum singular value of B. ■

Suppose we run the experiment from $t = 0$ to $t = T \in [t_N, t_{N+1})$. Then, from (19) and (24), the cumulative energy-harvesting error $\sum_{k=1}^{N} e_D(k-1)$, which defines total energy leak (thus, energy efficiency), can be approximated s.t.

$$\begin{aligned} \sum_{k=1}^{N} e_D(k-1) &\approx \frac{1}{3} a_{\max}^2 \bar{\sigma}[B] \Delta t^3 \times \frac{t_N - t_0}{\Delta t} \\ &= \frac{1}{3} a_{\max}^2 \bar{\sigma}[B] (t_N - t_0) \Delta t^2 \end{aligned}$$

where Δt is the average of Δt_k. Thus, given the same operation time, the amount of energy leak will *quadratically* decrease as we speed up the update rate of $y(k)$. This means that, for instance, if we densify a 50-ms data stream $y(k)$ ten times either by using a certain 5-ms running smoothing filter or even simply by repeating previous data every 5 ms, the energy leak can be reduced by 99%. Here, note that such a densifying process (which is located at the "filter" block in Fig. 3) will not jeopardize the passivity of the PSPM (see the paragraph after Fig. 3). Of course, for passivity, this densifying process (particularly, duplication) should be applied only to the data stream of $y(k)$ and not that of $\Delta E_y(k)$. Also, note that the boundedness assumption of $\ddot{x}(t)$ for Lemma 2 is likely to hold in most practical cases, particularly with the passivity-enforcing PSPM.

Remark 1: The assumption that $B\dot{x}(t)$ and $Kx(t)$ in (5) are continuous has been removed in [35]: If we use the sampled-data version of (5) s.t.

$$\tau(t) = -B \frac{x_k - x_{k-1}}{\Delta t_{k-1}} - K(x_k - \bar{y}(k)), \qquad t \in I_k$$

where $B = \mathrm{diag}[b_1, \ldots, b_n]$, $K = \mathrm{diag}[k_1, \ldots, k_n]$, $\Delta t_k := t_{k+1} - t_k$, and $x_k := x(t_k)$, the PSPM still enforces passivity (item 1 of Theorem 1) if the following condition holds:

$$b_{\mathrm{dev}}^i \geq b_i + \frac{b_i}{2} \left[1 + \frac{\Delta t_k}{\Delta t_{k-1}} \right] + \frac{k_i\, \Delta t_k}{2}$$

where b_{dev}^i is the (real) device damping along the x_i-direction.

Even so, we believe that the continuous-controller assumption for (5) is not so unreasonable here, since this paper (and our development of the PSPM) mainly focuses on the cases where the update rate of $y(k)$ is much slower (or only sparse) than the robot's local servo rate. This is further supported by the fact that the experiments of Sections IV and V run exactly as predicted by the theory that is derived with this continuous-controller assumption.

IV. Example: Bilateral Teleoperation Over the Internet

We apply the PSPM framework to the bilateral teleoperation over the Internet, with substantial varying delay and packet loss. For this problem, many schemes have been proposed, yet to our knowledge, for all of them, either theoretical guarantee of passivity is missing, particularly with varying delay/packet loss (e.g., [6] and [18]), and/or the fundamental position coordination is not ensured, particularly with packet loss (e.g., position drift [5], [19], [20]). In contrast, as shown later, both theoretically and experimentally, our PSPM framework guarantees (two-port closed-loop) passivity, regardless of how unreliable the Internet communication is, and it also enforces the master–slave position coordination, while complying with the passivity requirement.

We implement the PSPM in the master's and slave's sides individually, with the set position and the energy-shuffling terms being exchanged between them over the Internet. Then, by extending Theorem 1, we have the following proposition, which summarizes properties/performance of this PSPM-based Internet teleoperation, where $\star_1, \star_2$ (or $\star^1, \star^2$), respectively, represent variables for the master's and slave's sides.

Proposition 1: Consider master and slave robots, with each having open-loop dynamics of (1) and communicating over the Internet. Suppose we implement local spring–damper control (5) and the PSPM in Algorithm 1 for each of them individually. Further, suppose that there are no duplicated data receptions, and $x_i(t), \dot{x}_i(t)$ are continuous $\forall t \geq 0$, $i = 1, 2$.

1) *Passivity/stability:* The closed-loop teleoperator is two-port passive: $\forall T \geq 0$

$$\int_0^T [f_1^T \dot{x}_1 + f_2^T \dot{x}_2]dt \geq -d^2$$

where $d \in \Re$ is a bounded constant. Also, if the human operator and the slave environment are individually passive [i.e., each satisfying (18)], the interaction is stable in the sense of bounded $\dot{x}_i(t)$ $\forall t \geq 0$, $i = 1, 2$.

2) *Position coordination:* Assume that $f_1 = f_2 = 0$, and consider some unmodeled positive-definite dampings B_1^e, B_2^e for the master and slave robots. Also, assume that $\underline{\sigma}[M_i(x_i)]$ and $\partial M_{qr}^i(x_i)/\partial x_i^s$ satisfy the conditions of item 2 of Theorem 1. Then, $\dot{x}_i \to 0$, $\|\bar{y}_i(k+1) - \bar{y}_i(k)\| \to 0$, and $\|x_i(t) \to \bar{y}_i(k)\| \to 0$, $i = 1, 2$. Moreover, if $\exists p \geq 0$ s.t. $E_i(k) > 0$ $\forall k \geq p$, $i = 1, 2$, $\|x_1(t) - x_2(t)\| \to 0$.

3) *Force reflection:* Suppose $(\ddot{x}_i(t), \dot{x}_i(t)) \to 0$, $(x_1(t), x_2(t)) \to (x_o^1, x_o^2)$, and $\exists p \geq 0$ s.t. $E_i(k) > 0$ $\forall k \geq p$, $i = 1, 2$, where $x_o^1, x_o^2 \in \Re^n$ are constant vectors. Then

$$f_1(t) \to K_1(x_o^1 - x_o^2), \qquad f_2(t) \to K_2(x_o^2 - x_o^1) \tag{25}$$

where K_1, K_2 are the spring gains of (5) for the master's and slave's sides, respectively.

Proof: For the first item, summing the third and fourth lines of (19) for the master and the slave, we have that $\forall T \geq 0$, $\exists N_1, N_2 \geq 0$ s.t.

$$\begin{aligned}\int_0^T [f_1^T \dot{x}_1 + f_2^T \dot{x}_2]dt &\geq V(T) - V(0) + E(T) - E(0) \\ &\quad + \sum_{k=1}^{N_1} \Delta E_x^1(k) - \sum_{k=1}^{N_2} \Delta E_y^2(k) \\ &\quad + \sum_{k=1}^{N_2} \Delta E_x^2(k) - \sum_{k=1}^{N_1} \Delta E_y^1(k) \\ &\geq V(T) - V(0) + E(T) - E(0)\end{aligned} \tag{26}$$

where $V(t) := V_1(t) + V_2(t)$, with $V_i(t) = \kappa_i(t) + \bar{\varphi}_i(t)$, $E(T) := E_1(N_1) + E_2(N_2)$, $E(0) := E_1(0) + E_2(0)$, and we use the no-duplicated data-reception assumption:

$$\sum_{k=1}^{N_1} \Delta E_x^1(k) \geq \sum_{k=1}^{N_2} \Delta E_y^2(k), \qquad \sum_{k=1}^{N_2} \Delta E_x^2(k) \geq \sum_{k=1}^{N_1} \Delta E_y^1(k). \tag{27}$$

That is, $\Delta E_y^2, \Delta E_y^1$ are mere receptions of $\Delta E_x^1, \Delta E_x^2$. This proves two-port passivity, with $d^2 := V(0) + E(0)$. Boundedness of $\dot{x}_i(t)$ with passive human and slave environment can also be deduced from (26), with its LHS bounded by $c_1^2 + c_2^2$, where c_1, c_2 are c of (18) for the human and the environment.

For the second item, from (26), we have that for all $T \geq 0$

$$\int_0^T [f_1^T \dot{x}_1 + f_2^T \dot{x}_2]dt \geq V(T) - V(0) + E(T) - E(0) + \int_0^T \|\dot{x}_1\|_{B_e^1}^2 \, dt + \int_0^T \|\dot{x}_2\|_{B_e^2}^2 \, dt$$

with $f_1 = f_2 = 0$. This shows that $\dot{x}_i$ is bounded and square-integrable, as well as that $\|x_i(t) - \bar{y}_i(k)\|$ is bounded for all $t \geq 0$, $i = 1, 2$. Then, using the same argument as for item 2 of Theorem 1, we can show that $\dot{x}_i(t) \to 0$ and $\|x_i(t) - \bar{y}_i(k)\| \to 0$. Also, if $E(k) > 0$ for all $k \geq p$, then $\|x_i(t) - y_i(k)\| \to 0$ [since $\bar{y}_i(k) \to y_i(k)$], and $\|x_j(t) - y_i(k)\| \to 0$ [since $y_i(k)$ is the sampling of $x_j(t)$, with $\dot{x}_j(t) \to 0$ and (4)], $(i, j) = \{(1, 2), (2, 1)\}$. Thus, we have that

$$\|x_i(t) - x_j(t)\| \leq \|x_i(t) - y_i(k)\| + \|x_j(t) - y_i(k)\| \to 0.$$

The third item can also be proved by using the same argument for item 3 of Theorem 1 and condition (4), where the latter ensures that $y_j(k) \to x_o^i$, $(i, j) = \{(1, 2), (2, 1)\}$. ■

Note that the assumption of Theorem 1 that $\sum_{j=1}^k \Delta E_y(j) < b^2$ (i.e., energy supply from $\Delta E_y(k)$ is bounded) is not necessary here, since, with no data duplication, the master–slave energy shuffling defines passive-energy transmission on its own, i.e., from (27)

$$\sum_{k=1}^{N_1} \Delta E_x^1(k) + \sum_{k=1}^{N_2} \Delta E_x^2(k) \geq \sum_{k=1}^{N_1} \Delta E_y^1(k) + \sum_{k=1}^{N_2} \Delta E_y^2(k)$$

where the LHS is the energy injection into the communication, while the right-hand side (RHS) is the possible energy extraction. This also means that the severer the packet-loss rate becomes, the worse the energy efficiency (and performance) will be. How to predict/improve energy efficiency in the presence of packet loss, particularly when its probabilistic property is known, is a very interesting problem, and this is a topic for future work.

Here, we can also establish the boundedness of $\|x_1(t) - x_2(t)\|$ by applying Lemma 1 to the master's side. This is because item 1 of Lemma 1 requires only $\dot{x}_1(t)$ to be bounded (see proof of Lemma 1), which is granted by item 1 of Proposition 1. Also, similar to the argument after (21), with $\dot{x}_2(t)$ and $\|x_2(t) - \bar{y}_2(k)\|$ being bounded from (26) and with the conditions of item 2 of Lemma 1, $\ddot{x}_2(t)$ is also bounded. Thus, we can find $y_*(t)$ of item 2 of Lemma 1 for the master's side. Moreover, as shown in the experiments that are described later, with the human keeping injecting energy into the system, we would likely have that $\alpha_k < 1 - \epsilon_\alpha$, which implies that item 2 of Lemma 1 would also hold here (with its condition v also granted).

We perform an experiment using Phantom Desktop as a master and Phantom Omni as a slave, with both running at 1-ms local servo rate. A simple probabilistic model is used separately to simulate the forward (i.e., master to slave) and backward (i.e., slave to master) Internet communication. To avoid back-and-forth motion, we discard time-swapped $y_i(k)$. Also, if we have more than two set-position data available within a 5-ms window, we use only one of them (e.g., oldest), wait for 5 ms, and use another (or new data, if received in the meantime) to make the local servo rate (i.e., 1 ms) be faster than the set-position update (which is ≥5 ms here). Although this "slow-down" process can be avoided altogether by using Remark 1, we believe that it still reasonably well approximates the continuous assumption of $B\dot{x}(t), Kx(t)$ for (5), as supported by the fact that the system behaves exactly as predicted by the theory that is derived with this assumption in the experiments. Even if we discard $y_i(k)$, we still retain $\Delta E_y^i(k)$ and add it to $E_i(k)$ (without invoking PSPM) to improve energy efficiency. Here, note that the handling of $y_i(k), \Delta E_y^i(k)$, as stated previously, does *not* affect passivity of the PSPM.

After this, the following characteristics are achieved for the forward (or backward, respectively) communication: Delay (from sending to receiving a datum, as measured by a common clock) randomly varies from 0.1 to 0.48 s (or from 0.11 to 0.56 s, respectively); update interval I_k randomly varies from 1.2 to 198.5 ms (or from 1.2 to 223.6 ms, respectively); and packet-loss rate is 93.31% (or 92.15%, respectively). For the PSPM, we use the following parameters: $(B_1, K_1, E_1(0), \bar{E}_1) =$(5 N·s/m, 100 N/m, 0.015 N·m, 0.03 N·m) for the master; and $(B_2, K_2, E_2(0), \bar{E}_2)=$ (5 N·s/m, 50 N/m, 0.015 N·m, 0.03 N·m) for the slave. Here, since the master and slave devices are different, we choose different PSPM parameters for them. This is possible here due to the PSPM's locality (see the paragraph after Algorithm 1). We also install a wall in the slave environment (around $x_2 = -4$ mm).

The experimental results are shown in Fig. 5, where we can see 1) interaction stability between the human, the wall, and the closed-loop teleoperator over the Internet, with varying delay/packet loss (i.e., item 1 of Proposition 1); 2) position coordination outside the wall (i.e., item 2 of Proposition 1); and 3) force reflection during the hard contact (i.e., item 3 of Proposition 1, with $K_1 = 2K_2$). Note that the (commanding) human operator keeps injecting energy into the system via $f_1^T \dot{x}_1$. This energy is then captured by the energy reharvesting; it charges E_1 to $\bar{E}_1$, and, thenceforth, shuffles to the slave's side (around 11.5 s), thus resulting in an increase of E_2 around 12 s (after E_2's initial plunge to drive the slave to follow the master). During the hard contact, E_2 decreases. This energy from E_2 is mainly consumed to deform the slave PSPM spring K_2 and the wall, and when the contact is removed, it flows back to E_2 (around 30 s). Here, note that even if E_2 depletes during a hard contact, the perception of the wall at x_w would not be compromised much. This is because in this case, with $E_2 = 0$, x_2 will stuck with $x_2 \approx x_w$, and thus, $\bar{y}_1(k+1) = \bar{y}_1(k) \approx x_w$. This implies that the human user will still be able to perceive the wall at x_w, with the stiffness K_1.

We also implement a 5-ms running smoothing low-pass filter at the "filter" block in Fig. 3. See Fig. 6, where we can observe 1) smoother master/slave forces (small sharp jumps in τ_2 are due to the stiction-like behavior because of the device's Coulomb friction, which becomes more dominant here than in Fig. 5 as the operation slows down); 2) slower response due to the filter time lag [e.g., longer operation time and higher τ_1 during free motion due to sluggish $y_1(k)$]; and 3) much better energy-reharvesting

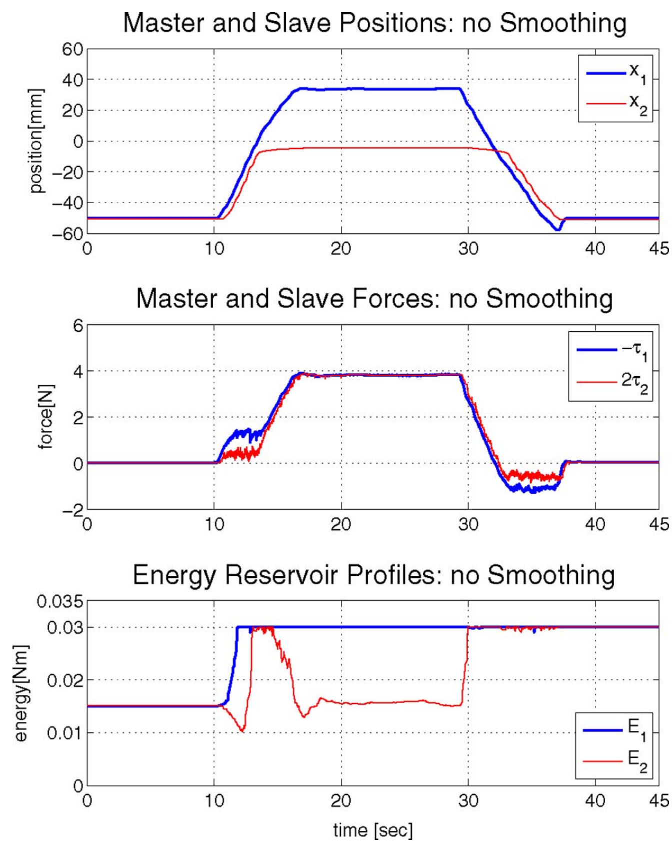

Fig. 5. Teleoperation over the Internet.

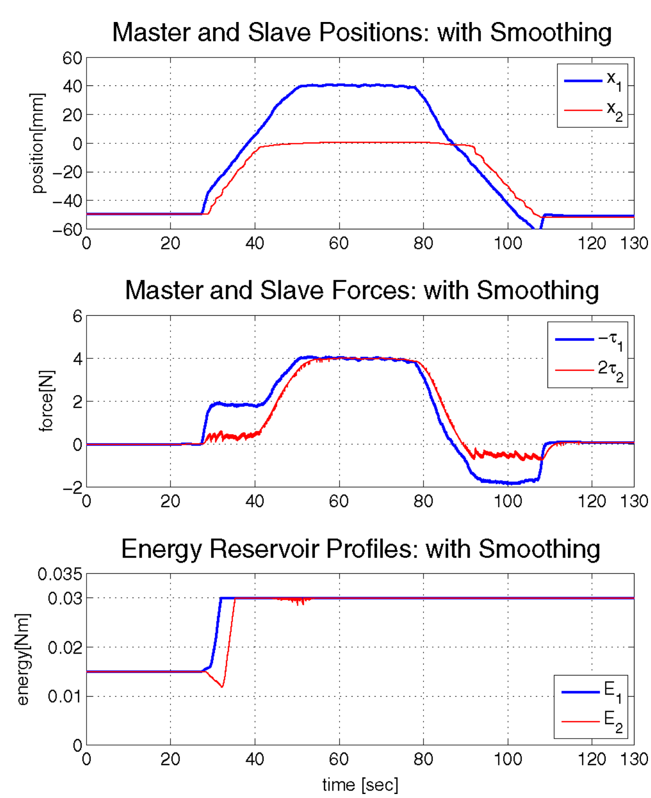

Fig. 6. Teleoperation with a smoothing filter.

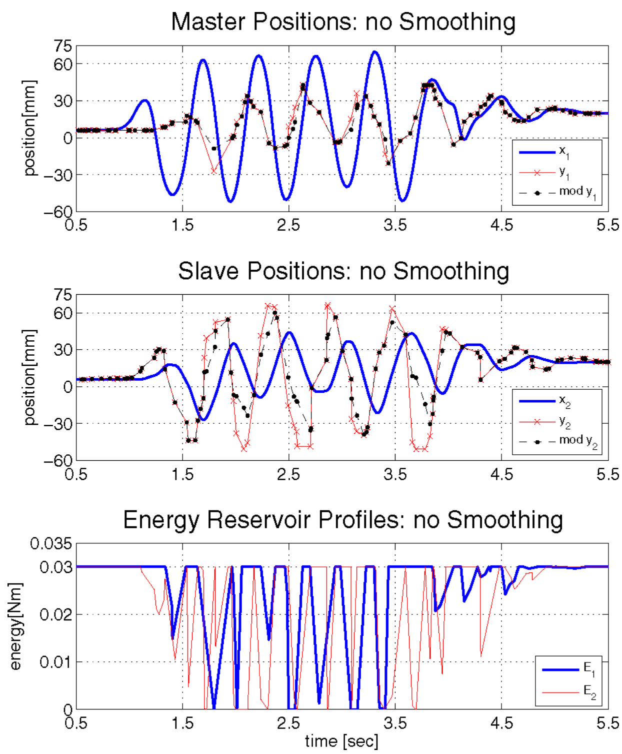

Fig. 7. Passifying/stabilizing action of PSPM.

efficiency (e.g., decrease of E_2 during the contact almost fully compensated by reharvested energy both from the master's and the slave's sides).

Note that $E_i(k) > 0$ in Figs. 5 and 6. Then, one may argue what is the benefit of using PSPM, since here, even if we use $\bar{y}_i(k) = y_i(k)$ without PSPM, the system will be stable. For this, we performed another experiment where we intentionally tried to destabilize the system (yet, failed)—see Fig. 7, where $\times$ and $\bullet$, respectively, denote $y_i(k)$ and $\bar{y}_i(k)$. There, we can see that when the system starts to behave too aggressively (i.e., reaching passivity/stability margin), the PSPM kicks in [i.e., $E_i(k) = 0$ with less aggressive $\bar{y}_i(k) \neq y_i(k)$] to enforce passivity (and stability). We believe that, along with its explicit position feedback (unlike, e.g., [5] and [20]), this "selective" activation of the PSPM is the main reason of its superior performance than other "static" works, where (conservatively designed) the passifying action is blindly applied all the time (e.g., [5], [6], and [18]).

Here, we choose the PSPM parameters, i.e., $B_i, K_i, E_i(0), \bar{E}_i$, with the following guidelines.

1) Choose K_i to be as large as possible (under the condition of Remark 1) for sharp perception/tracking.
2) Choose B_i to be small as possible for motion agility, yet not so small to avoid oscillatory behavior.
3) Choose $E_i(0)$ to be small (since energy reharvesting/shuffling will charge them), yet not so small to avoid the initial-takeoff problem.
4) Choose $\bar{E}_i$ to be small for being sensitive to energy shuffling, yet not so small to avoid frequent depletions of $E_i(k)$.

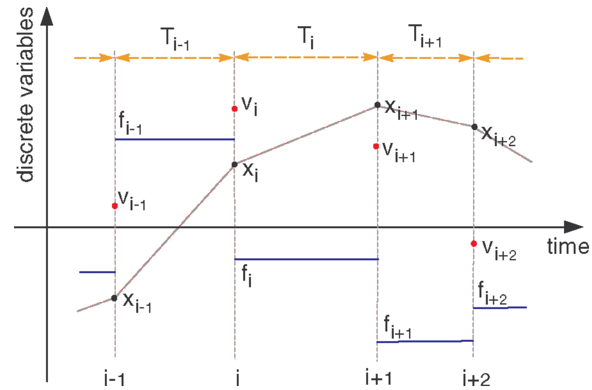

Fig. 8. Data update in discrete numerical integration.

However, tuning of these parameters is application-specific and should also be done with consideration of the characteristics of communication and/or filtering (e.g., for very sparse $y_i(k)$, large K_i is not desirable; yet, with a prediction filter, large K_i is desired, etc.).

V. Example: Slow and Variable-Rate Haptics

In this section, we apply the PSPM to the case of (impedance-causality) haptics, where the data update from the virtual world is slow w.r.t. the haptic-device servo rate and, possibly, of variable rate. This may happen when the complexity of the virtual world is high and time-varying (e.g., large-scale deformable object with intermittent contact [8]) and/or communication between the virtual world and the device is unreliable (e.g., a virtual world on a remote server that is connected via the Internet).

Now, suppose that the virtual world is guaranteed to well-behave (e.g., stable). Then, the PSPM that is implemented on the device's side will provide interaction stability, and items 2 and 3 of Theorem 1 will adequately characterize the system's performance (i.e., position coordination/force reflection). To achieve this well-behavedness, we again utilize the concept of passivity. More precisely, let us introduce a virtual mass (or proxy) that represents the presence of the haptic device in the (discrete) virtual world, whose evolution is given by a discrete integrator map $\mathcal{L}$

$$\mathcal{L} : (x_k, v_k, \tau_k, f_k) \rightarrow (x_{k+1}, v_{k+1})$$

where $x_k, v_k \in \Re^n$ are the position/velocity of the virtual mass at the kth discrete-time index ($k = 0, 1, \ldots$), $\tau_k, f_k \in \Re^n$ are its control (which are to be designed later), and interaction force from the virtual environment that surrounds it (e.g., contact force with a virtual wall), and x_{k+1}, v_{k+1} are the position/velocity updates after the integration step T_k (see Fig. 8).

Obviously, we want the position x_k of the virtual mass $\mathcal{L}$ to be as close to the position $x(t)$ of the device (1) as possible. For this, similar to $y(k)$ in Section III, we assume that at the onset of T_k, the virtual mass $\mathcal{L}$ receives the desired set position $y_k \in \Re^n$ from device (1), whose update may be of variable rate and whose transmission may have undergone varying delay, loss, time swapping, etc. We further assume that, similar to

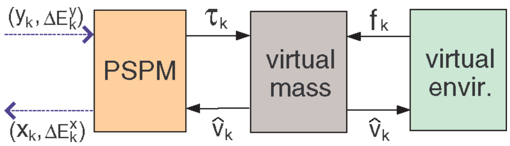

Fig. 9. PSPM implementation of the virtual world.

its (continuous) counterpart (1), the (discrete) virtual mass $\mathcal{L}$ possesses the following properties.

1) Similar to (5), we can design (discrete) τ_k to connect y_k and x_k, with damping dissipation $D_k := \|\hat{v}_k\|^2_{B_2} T_k$, and potential energy $\bar{\varphi}_k := (1/2)\|x_k - \bar{y}_k\|^2_{K_2} \geq 0$, where $B_2, K_2 \in \Re^{n \times n}$ are symmetric/positive-definite damping and spring matrices in the virtual world, $\bar{y}_k$ is the modulation of y_k (which is to be defined later), and $\hat{v}_k$ is a certain function of $v_1, \ldots, v_k, v_{k+1}$ (e.g., $\hat{v}_k = v_k$ [36], $\hat{v}_k = (v_{k+1} + v_k)/2$ [37]).
2) Similar to (6), with this coupling control τ_k, the virtual mass $\mathcal{L}$ is *discrete-time passive*: For all $k \geq 0$

$$f_k^T \hat{v}_k T_k = \kappa_{k+1} + \bar{\varphi}^-_{k+1} - \kappa_k - \bar{\varphi}_k + \|\hat{v}_k\|^2_{B_2} T_k \quad (28)$$

where $\kappa_k \geq 0$ is a certain positive-definite function suitably defined to describe the kinetic energy of $\mathcal{L}$, and $\bar{\varphi}^-_{k+1} := (1/2)\|x_{k+1} - \bar{y}_k\|^2_{K_2}$, which is similar to $\bar{\varphi}(t_k^-)$ in (10).

Then, by adding (28) for $T_o, T_1, \ldots, T_N$, we have that $\forall N \geq 0$

$$\sum_{k=0}^{N} f_k^T \hat{v}_k T_k = V_{N+1} - V_o - \sum_{k=1}^{N} \Delta\bar{P}_k + \sum_{k=0}^{N-1} D_k + D_N \quad (29)$$

where $V_{N+1} := \kappa_{N+1} + \bar{\varphi}^-_{N+1}$, $V_o := \kappa_o + \bar{\varphi}_o$, and

$$\Delta\bar{P}_k := \bar{\varphi}_k - \bar{\varphi}^-_k = \frac{1}{2}\|x_k - \bar{y}_k\|^2_{K_2} - \frac{1}{2}\|x_k - \bar{y}_{k-1}\|^2_{K_2}$$

i.e., spring energy jump at the onset of T_k is similar to (10).

Comparing (29) with (9), we can see that the (discrete-time passive) virtual mass $\mathcal{L}$ with the control τ_k essentially has the same energetics as the (continuous) haptic device with the local control (5). Thus, we can use the same PSPM in Algorithm 1 for the discrete virtual world as well: At the onset of T_k, given $(y_k, \Delta E^y_k, \bar{y}_{k-1}, E_{k-1}, D_{k-1})$, compute $(\bar{y}_k, \Delta E^x_k)$ by solving Algorithm 1, where E_k is the virtual energy reservoir, and $\Delta E^y_k, \Delta E^x_k$ are the energy-shuffling terms to/from the virtual world (see Fig. 9). Here, since we can compute the exact value of $D_{k-1} = \|\hat{v}_{k-1}\|^2_{B_2} T_{k-1}$, the approximation $D_{\min}$ in (13) is not necessary, thus implying no energy leak of the energy reharvesting for the virtual world (cf., Lemma 2).

With this discrete-time passivity of $\mathcal{L}$ and the PSPM installed in the virtual world, we can now theoretically guarantee the well-behavedness of the virtual world (and, subsequently, that of the total haptic system), as given by the following *two-port hybrid passivity*. For Proposition 2, we use the notations of Section III for variables of the device side, while $\star_k$ for those of the virtual world at the time index k.

Proposition 2: Consider the haptic device (1) with the control (5) and the virtual mass $\mathcal{L}$ with the control τ_k that satisfy the aforementioned two properties. Suppose that we individually implement the PSPM for the device's and virtual-world sides. Assume that $x(t), \dot{x}(t)$ are continuous $\forall t \geq 0$ and that there is no duplicated data reception. Then, the closed-loop haptic system is two-port hybrid passive: $\forall T \geq 0$, $\exists N_2 \geq 0$ s.t.

$$\int_0^T f^T \dot{x}\, dt + \sum_{k=0}^{N_2} f_k^T \hat{v}_k T_k \geq -d^2$$

where $d \in \Re$ is a bounded constant, and N_2 is defined s.t. $T_{N_2} \in [0, T)$, but $T_{N_2+1} \notin [0, T)$, i.e., the (virtual-world) integration step T_{N_2} occurs completely during the (real-world) time interval $[0, T)$, yet this is not true for T_{N_2+1}.

Proof: Similarly to (19), from (29), we have that $\forall T \geq 0$, $\exists N_2 \geq 0$, as defined previously, s.t.

$$\sum_{k=0}^{N_2} f_k^T \hat{v}_k T_k = V_{N_2+1} - V_o + \sum_{k=1}^{N_2} [D_{k-1} - \Delta\bar{P}_k] + D_{N_2}$$

$$\geq V_{N_2+1} - V_o + \sum_{k=1}^{N_2} [E_k - E_{k-1} - \Delta E^y_k + \Delta E^x_k]$$

where $V_{N_2+1} := \kappa_{N_2+1} + \bar{\varphi}^-_{N_2+1}$, $V_o := \kappa_o + \bar{\varphi}_o$, and the last line is due to the fact that $D_{N_2} \geq 0$ and the PSPM algorithm, i.e., similar to (20):

$$E_k = E_{k-1} + \Delta E^y_k + D_{k-1} - \Delta\bar{P}_k - \Delta E^x_k$$

where $\Delta E^x_k \geq 0$, with $\Delta E^x_k = 0$ only if line 8 of Algorithm 1 is false. Then, combining this inequality with (19), we can show that $\forall T \geq 0$, $\exists N_1 \geq 0$ s.t. $T \in I_{N_1} = [t_{N_1}, t_{N_1+1})$ and $\exists N_2 \geq 0$, as defined previously,

$$\int_0^T f^T \dot{x}\, dt + \sum_{k=0}^{N_2} f_k^T \hat{v}_k T_k \geq V(T) - V(0) + E(T) - E(0) + V_{N_2+1} - V_o + E_{N_2} - E_o \quad (30)$$

where $V(t) = \kappa(t) + \bar{\varphi}(t)$, and we use the no-duplicated data-reception assumption

$$\sum_{k=1}^{N_1} \Delta E_x(k) \geq \sum_{k=1}^{N_2} \Delta E^y_k, \qquad \sum_{k=1}^{N_2} \Delta E^x_k \geq \sum_{k=1}^{N_1} \Delta E_y(k)$$

which is similar to (27). Two-port hybrid passivity then follows from (30), with $d^2 := V(0) + E(0) + V_o + E_o$. ■

A direct consequence of this two-port hybrid passivity is that, similar to item 1 of Proposition 1, from (30), if the human is (continuous-time) passive [see (18)] and the virtual environment is (discrete-time) passive (i.e., $\exists\, c_2 \in \Re$ s.t. $\sum_{k=0}^{N} f_k^T \hat{v}_k T_k \leq c_2^2$ $\forall N \geq 0$), haptic interaction is stable in the sense of bounded $\dot{x}(t)$ and v_k (if κ_k is quadratic w.r.t. v_k—see below). Also, with this well-behaved virtual world, items 2 and 3 of Theorem 1 become applicable to the device's side, thereby providing theoretical guarantees of the system's haptic performance (under the conditions of Theorem 1).[3] Moreover, following the same argument of the second paragraph after Proposition 1, Lemma 1 can also be applied to the device's side to establish the boundedness of $\|x(t) - x_k\|$.

Note that the discrete-time passivity of $\mathcal{L}$ [see (28)] is crucial for the two-port passivity of our PSPM-based haptic rendering. However, this is also true for the well-known virtual coupling [7], since both the PSPM and the virtual coupling enforce passivity of only the (hybrid) coupling between the haptic device and the virtual mass, whereas the two-port passivity (of the total system) also requires individual passivity of the device and the virtual mass. Of course, as shown in [36], there is no integrator that is explicit (i.e., (x_{k+1}, v_{k+1}) solely depend on (x_k, v_k) and, thus, can be simulated fast) *and* passive (with supply rate $f_k^T v_k T_k$). This is the reason why the separation between the virtual-world design and the device servo loop, which requires passivity of $\mathcal{L}$, was just alluded to in [7] yet has not been fully materialized since then. However, the work in [36] does not rule out an integrator $\mathcal{L}$, which is implicit, yet still noniterative (thus, can still be simulated haptically fast), and/or passive with the supply rate other than $f_k^T v_k T_k$.

Recently, we have proposed such an implicit noniterative passive integrator [37], which can be written for this paper as

$$\mathcal{L}_{\rm dp} : M_2 \frac{v_{k+1} - v_k}{T_k} = \tau_k + f_k, \qquad \frac{v_{k+1} + v_k}{2} = \frac{x_{k+1} - x_k}{T_k}$$

with the coupling control

$$\tau_k = -B_2 \frac{v_{k+1} + v_k}{2} - K_2 \left(\frac{x_{k+1} + x_k}{2} - \bar{y}_k \right)$$

where $M_2, B_2, K_2 \in \Re^{n \times n}$ are, respectively, symmetric/positive-definite mass, damping, and spring matrices. It can then be shown that this $\mathcal{L}_{\rm dp}$ possesses discrete-time passivity [see (28)] (and other properties stated there), with $\kappa_k := (1/2)\|v_k\|_{M_2}^2$, and $\hat{v}_k := (v_{k+1} + v_k)/2$. Here, note that the passivity of $\mathcal{L}_{\rm dp}$ depends not only on the choice of $\hat{v}_k$ (which is also adopted in [20]) but on the specific structure of $\mathcal{L}_{\rm dp}$ as well. For more details, see [37].

We use this $\mathcal{L}_{\rm dp}$ for the experiment, with T_k (which is synchronized with the real-world clock) randomly varying from 10 to 50 ms. We also implement a spring–damper-type unilateral virtual wall and use the noniterative passive-wall-rendering algorithm (see [37] for more details) to enforce passivity of this virtual wall (i.e., bounded $\sum f_k^T \hat{v}_k T_k$). For $\mathcal{L}_{\rm dp}$, we set $M_2 = 0.001$ kg, while, for the virtual wall, $K_w = 30$ kN/m and $B_w = 100$ N·s/m. We also use the following PSPM parameters: $(B_1, K_1, E(0), \bar{E})$ =(5 N·s/m, 200 N/m, 0.16 N·m, 0.2 N·m) for the device's side; $(B_2, K_2, E_o, \bar{E}_2)$ =(5 N·s/m, 500 N/m, 0.16 N·m, 0.2 N·m) for the virtual-world side. A Phantom Desktop is used as the haptic device with a 1-ms local servo rate.

Other than the variable T_k, we assume that the data update between the device and the virtual world is perfect: At each onset of T_k, $\mathcal{L}_{\rm dp}$ gets the device position $x(t)$ (and integrate $\mathcal{L}_{\rm dp}$ over T_k), while at each end of T_k, the device gets the virtual-mass position x_{k+1} [and apply it to the control (5)]. Note that neither time-swapping correction nor "slow-down" operation of Section IV is necessary here, since, although T_k is nonuniform, the integration of $\mathcal{L}_{\rm dp}$ always takes longer than 10 ms (which is much slower than 1 ms local servo rate) and is always forward in time as well. A PC with a 3.0-GHz DualCore CPU and 4 GB of RAM is used to run all the numerical algorithms, 3-D OpenGL graphics, and the haptic-device servo loop.

[3]In fact, we can prove items 2 and 3 of Proposition 1 for $\mathcal{L}_{\rm dp}$. Yet, we do not present them here and will report in a future publication, since doing so requires further theoretical development of $\mathcal{L}_{\rm dp}$, which is beyond the scope of this paper.

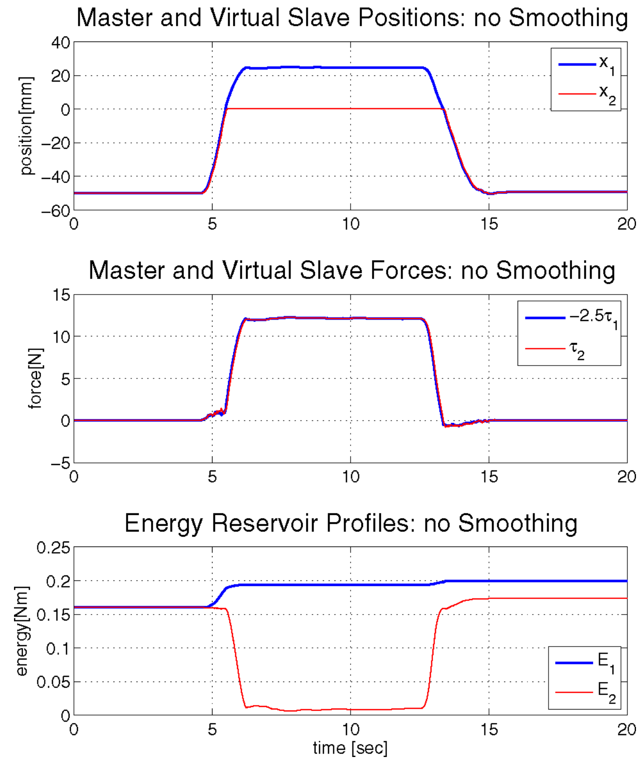

Fig. 10. Haptic experiment without smoothing.

The results are shown in Fig. 10, from which we can see passivity/stability and performance of the haptic interaction, even with slow and variable-rate data update, as predicted in Theorem 1 and Proposition 2. Since these results are very similar to those of Fig. 5, we omit detailed explanations here. We also perform the experiments that are similar to Figs. 6 (i.e., a smoothing filter) and 7 (i.e., passifying action of the PSPM) and achieve similar results (and thus, not shown here). Only exceptions for this similarity are 1) the stiction-like behavior of the slave in Fig. 6 is now gone, since the virtual world does not have Coulomb friction, and 2) the smoothing effect is less prominent, since a) data-update rate is overall much denser here (i.e., 10 ms $\leq T_k \leq$ 50 ms) than for the teleoperation (i.e., 5 ms $\leq I_k \leq$ 198.5/223.6 ms), and b) energy leaks occur only in the device's side (cf., Lemma 2).

A very interesting aspect of our framework is that the parameters of the virtual world (e.g., T_k, M_2, B_w, K_w) can be chosen independently from the device servo-loop parameters and damping. For instance, we can set M_2 to be arbitrary small, without being restricted by the minimum-mass condition [36]. In fact, roughly computed minimum mass of [36] is around 0.8 kg here, yet, we could use $M_2 = 0.001$ kg, thus enjoying a much sharper force reflection and a faster position coordination. This separation between the device servo loop and the virtual world, which was originally envisioned in [7], can be achieved here, because, with our PSPM and the passive integrator $\mathcal{L}_{\rm dp}$ [37], passivity of the haptic device, virtual environment, and the coupling between them are achieved individually.

Note that some other implicit/iterative passive integrators than $\mathcal{L}_{\rm dp}$ can also be used here, regardless of how slow they are, since the PSPM can accommodate arbitrarily slow data update. Also, note that even if $\mathcal{L}_{\rm dp}$ is used, if its data-update is either of variable rate or imperfect (e.g., delay/loss), the well-known virtual coupling [7] cannot theoretically enforce two-port hybrid passivity, since its supporting theory (e.g., [11]) does not allow such scenarios (see [35] for an extension to this case). In contrast, our PSPM framework can do so, since it requires only the data streams $y(k)$ and y_k to be a discrete sequence. Also, note from the plots that our PSPM exhibits no noisy behavior, which is often encountered with the PO/PC framework [13], [24] when the velocity becomes small/zero.

VI. Conclusion

In this paper, we propose a PSPM framework, which enables us to connect a (continuous-time) multi-DOF nonlinear robotic system to a sequence of (discrete-time) set-position signal $y(k)$ via a simple spring coupling with damping injection, while enforcing closed-loop passivity, thereby enhancing interaction stability/safety, while providing explicit position feedback. We present the algorithm of PSPM and theoretically/experimentally show its passivity and performance characteristics, particularly for the two important applications: Internet teleoperation with packet loss/varying delay and haptics with slow/variable-rate data update.

The PSPM has some unique properties/flexibilties, which would be useful for some applications and deserve more exploration, in particular 1) intermediate data processing (at "filter" block in Fig. 3) to enhance system's performance (e.g., predictive display and estimator), while enforcing passivity, thereby possibly challenging the presumption that passivity implies poor performance (see [38] for a similar idea of "passivity layer") and 2) locality of the PSPM for applications where scalability is demanded, and the communication link is not always bilateral (e.g., a multiuser haptic collaboration over the Internet [39]). The PSPM may also handle with asynchronous data update among different DOF of (1) if it is reformulated with controller passivity [14] (and diagonal B, K).

References

[1] D. J. Lee and K. Huang, "Passive position feedback over packet-switching communication network with varying-delay and packet-loss," in *Proc. HAPTICS*, Reno, NV, Mar. 2008, pp. 335–342.

[2] D. J. Lee and K. Huang, "Passive set-position modulation approach for haptics with slow variable, and asynchronous update," in *Proc. HAPTICS*, Salt Lake City, UT, Mar. 2009, pp. 541–546.

[3] K. Huang and D. J. Lee, "Implementation and experiments of passive set-position modulation framework for interactive robotic systems," in *Proc. IEEE/RSJ Int. Conf. Intell. Robots Syst.*, St. Louis, MO, Oct. 2009, pp. 5615–5620.

[4] R. Oboe and P. Fiorini, "A design and control environment for Internet-based telerobotics," *Int. J. Robot. Res.*, vol. 17, no. 4, pp. 433–449, 1998.

[5] G. Niemeyer and J. J. E. Slotine, "Telemanipulation with time delays," *Int. J. Robot. Res.*, vol. 23, no. 9, pp. 873–890, 2004.

[6] D. J. Lee and M. W. Spong, "Passive bilateral teleoperation with constant time delay," *IEEE Trans. Robot.*, vol. 22, no. 2, pp. 269–281, Apr. 2006.

[7] J. E. Colgate, M. C. Stanley, and J. M. Brown, "Issues in the haptic display of tool use," in *Proc. IEEE/RSJ Int. Conf. Intell. Robots Syst.*, 1995, vol. 3, pp. 140–145.

[8] J. Barbič and D. L. James, "Six-dof haptic rendering of contact between geometrically complex reduced deformable models," *IEEE Trans. Haptics*, vol. 1, no. 1, pp. 1–14, Jan. 2008.

[9] J. E. Colgate, "Coupled stability of multiport systems—Theory and experiments," *ASME J. Dyn. Syst., Meas. Control*, vol. 116, no. 3, pp. 419–428, 1994.

[10] R. J. Anderson and M. W. Spong, "Bilateral control of tele-operators with time delay," *IEEE Trans. Autom. Control*, vol. 34, no. 5, pp. 494–501, May. 1989.

[11] J. E. Colgate and G. Schenkel, "Passivity of a class of sampled-data systems: Application to haptic interfaces," *J. Robot. Syst.*, vol. 14, no. 1, pp. 37–47, 1997.

[12] S. Stramigioli, *Modelling and IPC Control of Interactive Mechanical Systems: A Coordinate-Free Approach*. London, U.K.: Springer-Verlag, 2001.

[13] B. Hannaford and J.-H. Ryu, "Time domain passivity control of haptic interfaces," *IEEE Trans. Robot. Autom.*, vol. 18, no. 1, pp. 1–10, Feb. 2002.

[14] D. J. Lee and P. Y. Li, "Passive bilateral control and tool dynamics rendering for nonlinear mechanical teleoperators," *IEEE Trans. Robot.*, vol. 21, no. 5, pp. 936–951, Oct. 2005.

[15] G. Sankaranarayanan and B. Hannaford, "Experimental Internet haptic collaboration using virtual coupling schemes," in *Proc. HAPTICS*, Reno, NV, Mar. 2008, pp. 259–266.

[16] P. Y. Li and R. Horowitz, "Passive velocity field control of mechanical manipulators," *IEEE Trans. Robot. Autom.*, vol. 15, no. 4, pp. 751–763, Aug. 1999.

[17] D. J. Lee and P. Y. Li, "Passive bilateral feedforward control of linear dynamically similar teleoperated manipulators," *IEEE Trans. Robot. Autom.*, vol. 19, no. 3, pp. 443–456, Jun. 2003.

[18] N. Chopra, M. W. Spong, S. Hirche, and M. Buss, "Bilateral teleoperation over the internet: The time varying delay problem," in *Proc. Amer. Control Conf.*, 2003, pp. 155–160.

[19] P. Berestesky, N. Chopra, and M. W. Spong, "Discrete time passivity in bilateral teleoperation over the Internet," in *Proc. IEEE Int. Conf. Robot. Autom.*, 2004, pp. 4557–4564.

[20] S. Stramigioli, C. Secchi, A. van der Schaft, and C. Fantuzzi, "Sampled data systems passivity and discrete port-Hamiltonian systems," *IEEE Trans. Robot.*, vol. 21, no. 4, pp. 574–587, Aug. 2005.

[21] J. Ryu, D. Kwon, and B. Hannaford, "Stable teleoperation with time domain passivity control," *IEEE Trans. Robot. Autom.*, vol. 20, no. 2, pp. 365–373, Apr. 2004.

[22] J.-H. Ryu, Y. S. Kim, and B. Hannaford, "Sampled- and continuous-time passivity and stability of virtual environment," *IEEE Trans. Robot.*, vol. 20, no. 4, pp. 772–776, Aug. 2005.

[23] J.-P. Kim and J. Ryu, "Stable haptic interaction control using energy bounding algorithm," in *Proc. IEEE/RSJ Int. Conf. Intell. Robots Syst.*, 2004, pp. 1210–1217.

[24] J.-H. Ryu, B. Hannaford, D.-S. Kwon, and J.-H. Kim, "A simulation/experimental study of the noisy behavior of the time-domain passivity controller," *IEEE Trans. Robot.*, vol. 21, no. 4, pp. 733–741, Aug. 2005.

[25] C. Seo, J. Kim, J.-P. Kim, J. H. Yoon, and J. Ryu, "Stable bilateral teleoperation using the energy-bounding algorithm: Basic idea and feasibility tests," in *Proc. IEEE/ASME Int. Conf. Adv. Intell. Mechatronics*, 2008, pp. 335–340.

[26] J. E. Colgate and J. M. Brown, "Factors affecting the z-width of a haptic display," in *Proc. IEEE Int. Conf. Robot. Autom.*, 1994, pp. 3205–3210.

[27] J. Zhao and D. J. Hill, "Dissipasivity theory for switched systems," *IEEE Trans. Autom. Control*, vol. 53, no. 4, pp. 941–953, May. 2008.

[28] D. J. Lee, "Semi-autonomous teleoperation of multiple wheeled mobile robots over the internet," presented at the ASME Dyn. Syst. Control Conf., Ann Arbor, MI, Oct. 2008 (CD-Rom).

[29] R. S. Strichartz, *The Way of Analysis,* revised ed. Sudbury, MA: Jones & Bartlett, 2000.

[30] J. J. Abbott and A. M. Okamura, "Effects of position quantization and sampling rate on virtual-wall passivity," *IEEE Trans. Robot.*, vol. 21, no. 5, pp. 952–964, Oct. 2005.
[31] S. Boyd and L. Vandenberghe, *Convex Optimization*. Cambridge, U.K.: Cambridge Univ. Press, 2004.
[32] M. W. Spong, S. Hutchinson, and M. Vidyasaga, *Robot Modeling and Control*. Hoboken, NJ: Wiley, 2006.
[33] F. Bullo and R. M. Murray, "Tracking for fully actuated mechanical systems: A geometric framework," *Automatica*, vol. 35, pp. 17–34, 1999.
[34] D. Liberzon and A. S. Morse, "Basic problems in stability and design of switched systems," *IEEE Control Syst. Mag.*, vol. 19, no. 5, pp. 59–70, Oct. 1999.
[35] D. J. Lee, "Extension of Colgate's passivity condition to variable-rate haptics," in *Proc. IEEE/RSJ Int. Conf. Intell. Robots Syst.*, 2009, pp. 1761–1766.
[36] J. M. Brown and J. E. Colgate, "'Minimum mass for haptic display simulations," in *Proc. IMECE*, 1998, pp. 249–256.
[37] D. J. Lee and K. Huang, "On passive non-iterative variable-step numerical integration of mechanical systems for haptic rendering," presented at the ASME Dyn. Syst. Control Conf., Ann Arbot, MI, Oct. 2008 (CD-Rom).
[38] M. Franken, S. Stramigioli, R. Reilink, C. Secchi, and A. Macchelli, "Bridging the gap between passivity and transparency," presented at the Robot.: Sci. Syst. Conf., Seattle, WA, 2009.
[39] D. J. Lee and K. Huang, "Peer-to-peer control architecture for multiuser haptics collaboration over undirected delayed packet-switching network," in *Proc. IEEE Int. Conf. Robot. Autom.*, Anchorage, AK, to be published.

Dongjun Lee (S'02–M'04) received the B.S. degree in mechanical engineering and the M.S. degree in automation and design from the Korea Advanced Institute of Science and Technology, Daejeon and Seoul, Korea, in 1995 and 1997, respectively, and the Ph.D. degree in mechanical engineering from the University of Minnesota, Twin Cities, in 2004.

From 1997 to 1999, he was an Engine Development Engineer with Kia Motors Corporation, Korea. From 2004 to 2006, he was a Postdoctoral Research Fellow with the Coordinated Science Laboratory, University of Illinois, Urbana-Champaign. Since 2006, he has been an Assistant Professor with the Department of Mechanical, Aerospace and Biomedical Engineering, University of Tennessee, Knoxville. His current research interests include dynamics and control of robotic and mechatronic systems, with particular emphasis on teleoperation, haptics, multirobot systems, nonholonomic systems, and geometric-mechanics control theory.

Dr. Lee received the National Science Foundation Faculty Early Career Development (CAREER) Award in 2009. He was also a Doctoral Dissertation Fellow of the University of Minnesota during 2002–2003.

Ke Huang received the B.S. degree in automation from the University of Science and Technology of China, Hefei, China, in 2005. He is currently working toward the Ph.D. degree with the University of Tennessee, Knoxville.

His research interests include bilateral teleoperation over the Internet, multiagent distributed coordination, and multiuser haptic collaboration.